CHEMISTRY & BIODIVERSITY

Accepted Article

Title: Synthesis, cytotoxicity and antimicrobial evaluation of new coumarin-tagged β-lactam triazole hybrid

Authors: Sanjeev Dhawan, Paul Awolade, Prishani Kisten, Nosipho Cele, Ashona-Singh Pillay, Sourav Taru Saha, Mandeep Kaur, sreekanth b. Jonnalagaddas, and Parvesh Singh

To be cited as: *Chem. Biodiversity* 10.1002/cbdv.201900462

Link to VoR: http://dx.doi.org/10.1002/cbdv.201900462

Synthesis, cytotoxicity and antimicrobial evaluation of new coumarin-tagged β-lactam triazole hybrid

Sanjeev Dhawan[a], Paul Awolade[a], Prishani Kisten[a],Nosipho Cele, Ashona-Singh Pillay[a], SouravTaru Saha[b], Mandeep Kaur[b], Sreekantha B. Jonnalagadda[a] and Parvesh Singh[a]*

[a]School of Chemistry and Physics, University of KwaZulu-Natal, P/Bag X54001, Westville, Durban, South Africa-4000
[b]School of Molecular and Cell Biology, University of the Witwatersrand, Private Bag 3, Johannesburg, WITS-2050, South Africa
*Email address for correspondence: singh4@ukzn.ac.za, parveshdurban@gmail.com

Abstract:

A series of coumarin-tagged β-lactam triazole hybrids (**10a-o**) were synthesized and tested for their cytotoxic activity against MDA-MB-231 (triple negative breast cancer), MCF-7 (estrogen receptor positive breast cancer (ER+) and A549 cells (human lung carcinoma) cancer cell lines including a normal cell line, HEK-293 (human embryonic kidney). Two compounds, **10b** and **10d** exhibited substantial cytotoxic effect against MCF-7 cancer cell-line with IC_{50} values of 53.55 and 58.62 µM, respectively. More importantly, compounds **10b** and **10d** were non-cytotoxic against HEK-293 cells. Structure-activity relationship (SAR) studies suggested that the nitro and chloro group at the C-3 position of phenyl ring are favorable for anticancer activity, particularly against MCF-7 cell-line. Furthermore, antimicrobial evaluation of these compounds revealed modest inhibiton of examined pathogenic strains with compounds **10c** and **10i** being the most promising antimicrobial agents against *Pseudomonas aeruginosa* and *Candida albicans* respectively.

Keywords: β-Lactam, Coumarin, 1,2,3-triazole,MDA-MB-231, MCF7, HEK-293, Molecular hybridization.

Introduction

Cancer remains the most typical cause of death in many developed countries, with breast and lung adenocarcinomas being the most prevalent forms.[1,2]The adverse effects of combination chemotherapy, the most preferred method for cancer treatment, necessitates the development of new anticancer agents with acceptable toxicity profile and improved efficacy.[3] Similarly, bacterial infections pose an increasing community health issue and a consequential life-threatening risk to human existence due to the rising resistance to current antibiotics.[4] According to the World Health Organization (WHO) fact sheet 2018, approximately 500,000 people suffer from bacterial infections caused by *Klebsiella pneumoniae*, *Escherichia coli*, *Staphylococcus aureus*, *Streptococcus pneumoniae* and *Salmonella* species in over 22 countries. Therefore, there is an imperative requirement to establish new antimicrobial agents with potent activity against resistant microorganisms.[5]

Coumarin is a versatile scaffold that is widely distributed in nature with vast application in the field of medicinal chemistry. The synthetic accessibility of the coumarin scaffold enables it to become the perfect platform for structural modifications, and derivatisation.[6] Coumarin-based compounds have displayed a broad spectrum of pharmacological activity such as anti-viral,[7] anticancer,[8] anti-fungal,[9] anti-inflammatory[10] and anti-HIV.[11] Currently, a coumarin-based VEGF expression and angiogenesis inhibitor, NM-3 is under phase I clinical trials.[12] Nevertheless, only a few synthetic coumarin derivatives have been used to perform antimicrobial characterisation, particularly those effective against gram-positive bacterial species.[13] Also, there has been a resurgent interest for coumarin-based antibiotics since their isolations from *Streptomyces* species. Notable examples include coumermycin, clorobiocin, as well as novobiocin which were identified as potent bacterial DNA gyrase and topoisomerase inhibitor.[14] For instance,

10.1002/cbdv.201900462

Damu *et al*. reported some coumarins possessing potent antibacterial activity against methicillin and ciprofloxacin-resistant *S. aureus* strains.[15] Similarly, Ghalehshahi *et al*. synthesized new coumarin analogues with superior antimicrobial activity when compared to their parent molecules.[16]

Furthermore, β-lactam antibiotics such as the classical cephalosporins, penicillins, non-classical monobactams and carbapenams due to their synthetic accessibility and low hepatotoxicity profile have played a vital role in treating bacterial infections.[17] So far, they remain the leading class of agents used in the antimicrobial regimen and have significantly enhanced human health and life expectancy.[18] However, pathogenic resistance has been a significant setback to the efficacious clinical utility of β-lactams.[19] Current research efforts are focused on the synthetic modifications of the β-lactam scaffold to afford compounds with enhanced antimicrobial and anticancer activity while prevailing against β-lactamase induced resistance. β-Lactams execute their antimicrobial properties *via* the disruption of interpeptide cross-links into bacterial peptidoglycan cell wall by inhibiting bacterial transpeptidases, termed penicillin-binding proteins (PBPs), thereby curbing rigidity of the bacterial cell wall.[20] Accordingly, Chen *et al*. reported that the β-lactam derivatives display their anticancer activity by inhibiting DNA replication thus influencing DNA damage and activating the apoptotic death program in human leukemic Jurkat T-cells. In addition, considering the structural flexibility of β-lactams, they have the potential to be developed into anticancer agents by various structural modifications.[21]

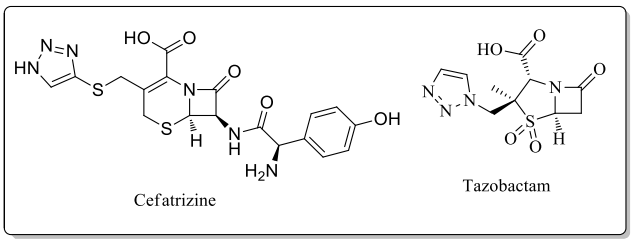

Figure 1.β-lactam tagged1,2,3triazole-based drugs in the market

Likewise, 1,2,3-triazole serve as an attractive heterocyclic group to connect two pharmacophores and biologically active fragments into one molecule to get progressive multifunctional compounds.[22-27] Moreover, the binding ability of 1,2,3-triazole framework with molecular targets due to their rigidity, high dipole moment, stability and capability to form hydrogen bonding under *in vivo* conditions has resulted in highly potent bioactive agents.[28,29]

In view of the aforementioned biological significance, we decided to fuse coumarin, β-lactam, and 1,2,3-triazole pharmacophoric units into a single architecture using the concept of molecular hybridisation.[30-33] The desired molecular conjugates were synthesised by using the Copper-assisted 1,3-dipolar cycloaddition reaction between the alkyne-substituted coumarins and azido lactams. All synthesized compounds were further tested *in vitro* against three cancer cell lines and microbial strains.

Results and discussion

Chemistry

The general synthetic routes employed in this study are depicted in **Schemes 1-2**. A novel series of triazole-linked coumarin-β-lactam (**10a-o**) molecular hybrids were prepared from **7**-(ethynyloxy)-4,5-dimethyl-2H-chromen-2-one (**9a)** and **7**-(ethynyloxy)-4-methyl-2H-chromen-2-one (**9b),** using various substituted azido lactams (**6**) in the presence of $CuSO_4.5H_2O$ and sodium ascorbate (as reducing agent) in Dichloromethane:Water (DCM:H_2O) (8:2) at room temperature.[34-35] The key starting materials **7**-hydroxy-4,5-dimethyl-2H-chromen-2-one (**8a**) and **7**-hydroxy-4-methyl-2H-chromen-2-one (**8b**) were prepared by the reaction of orcinol (**7a**) and phloroglucinol (**7b**), respectively with ethyl acetoacetate in sulfuric acid (Pechmann reaction).[36] 7-(Ethynyloxy)-4,5-dimethyl-2H-chromen-2-one **9a**, in turn, was prepared through the base-

promoted reaction of 7-hydroxy-4,5-dimethyl-2H-chromen-2-one **8a** with propargyl bromide in Dimethylformamide (DMF). Substituted azido lactams were prepared by using azido acetic acid **2** and an imine (**5a-h)** at 0-5ºC.[37] The key azidoketene intermediate was generated *in situ* in the presence of *p*-toluene sulfonyl chloride and triethylamine and subsequently converted to the desired azido lactams.

The precise structure elucidation of all newly synthesised compounds was accomplished on the basis of spectroscopic data (^{1}H NMR, ^{13}C NMR, COSY, HSQC, HMBC, IR and mass spectrometry). The details of spectroscopic data are shown in experimental data whereas the salient features of the representative compound are discussed here. For instance, the formation of compound **10a** was confirmed by a characteristic deshielded proton of its triazole ring that resonated at δ 7.84 ppm in its proton NMR. Moreover, a doublet of doublet (dd) at δ 5.90 for H_1, a doublet at 6.27 ppm for H_3 proton, and two singlets at δ2.33 and δ 2.17 ppm for methyl protons also confirmed the structure of **10a**. The HRMS spectrum of compound **10a** also exhibited its molecular ion peak of *m/z* 541.1850**,** and corroborated the proposed structure.

10.1002/cbdv.201900462

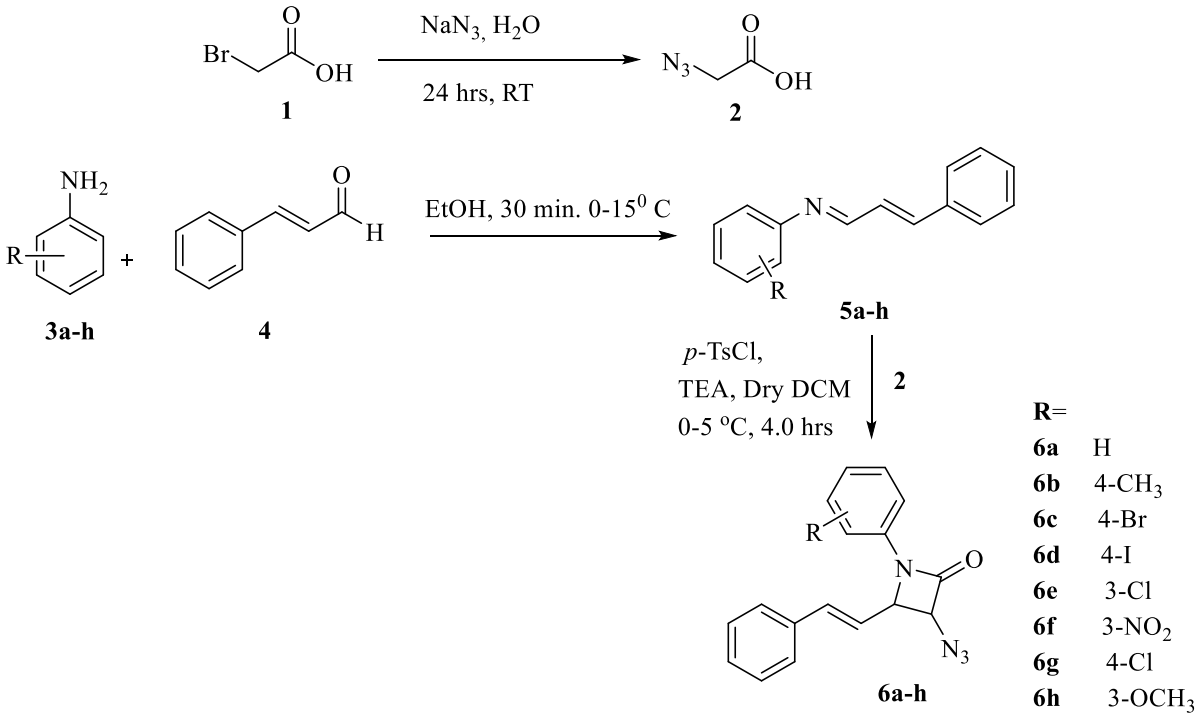

Scheme 1. Synthetic pathway to azido β-lactam derivatives

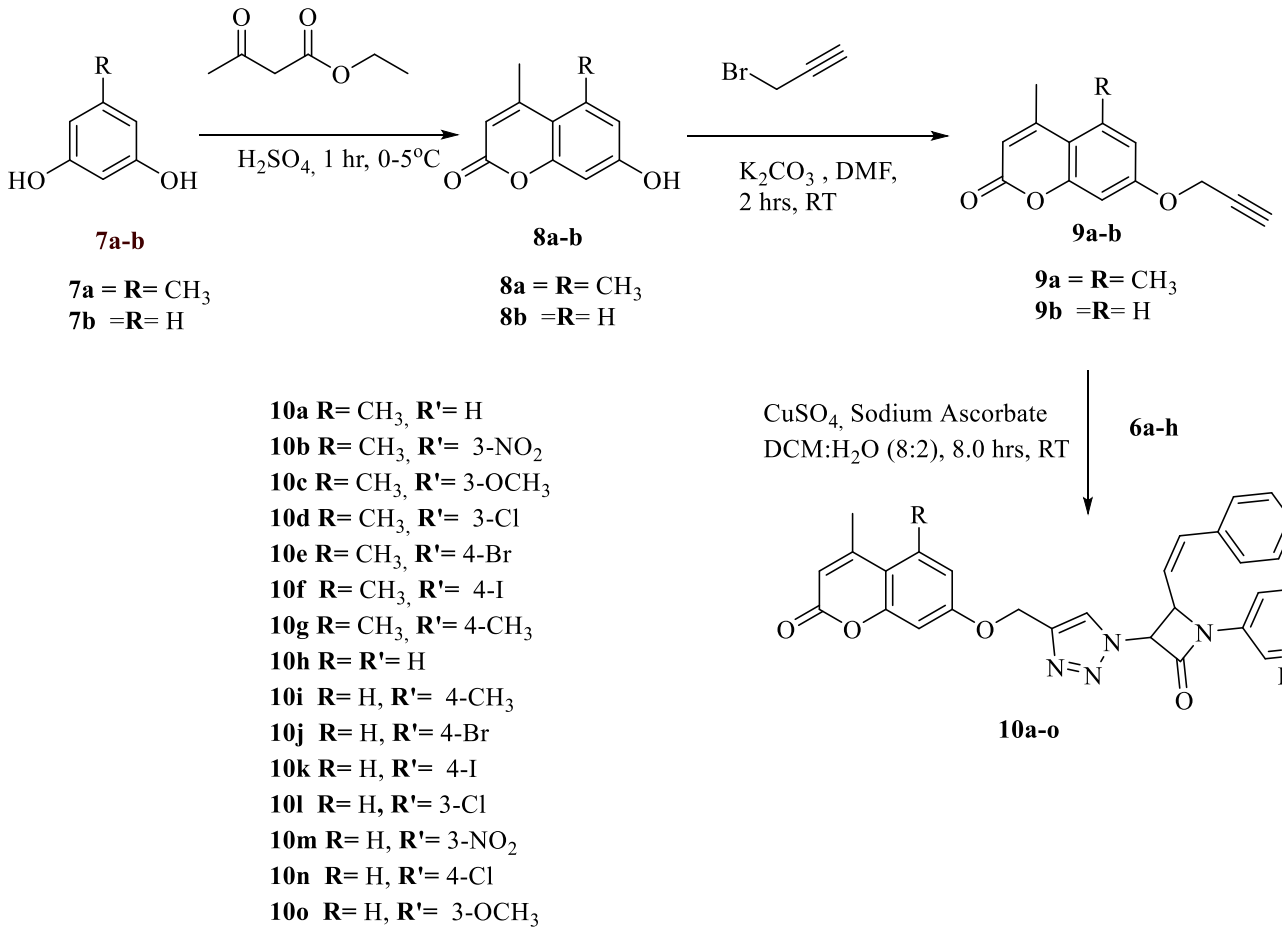

Scheme 2. Synthetic pathway to coumarin-β-lactam derivatives

Furthermore, the quaternary carbons in compound **10a** were identified based on the heteronuclear multiple bond correlation (HMBC) data, depicted in **Figure 2**. For instance, the carbon C-4a was identified based on its correlation with the CH_3-9 and CH_3-10 protons. Similarly, the carbon C-2 was distinguished by its HMBC with H-3; C-4a and C-8 with H-6, C-7 and C-6 with H-8 and finally C-6 was assigned based on its HMBC with CH_3-9, and H-8.

10.1002/cbdv.201900462

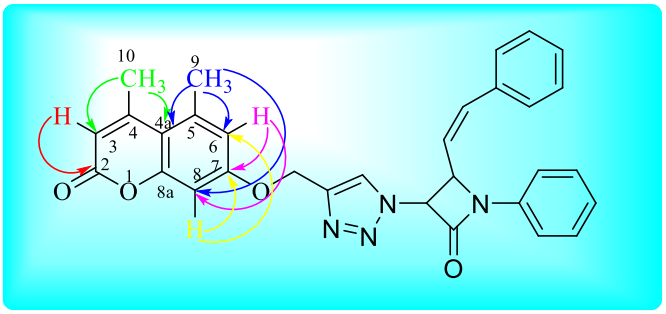

Figure 2. HMBC ($^{1}H \longrightarrow {}^{13}C$) spectrum of **10a** showing important correlations.

Anticancer evaluation

The cytotoxic efficacy of all synthesized compounds (**10a-g**, and **10h-o**) was tested against three cancer cell lines, namely MCF7 cells (human breast adenocarcinoma) (ER+), MDA-MB-231 cells (human breast adenocarcinoma) (TNBC) and A549 cells (Human lung carcinoma), including one normal cell-line HEK-293 (Human embryonic kidney), using an MTT (3-(4,5-Dimethylthiazol-z-yl)-2,5-diphenyltetrazolium bromide) assay **Table 1**.

Fig 3 to **7** illustrate the cytotoxicity results of selected compounds, whereas the IC_{50} value, which is the concentration required to inhibit 50% of cell viability by the test compounds, is summarised in **Table 1**. As observed in **Fig.3**, compound **10b** and **10d** appeared to be active against the MCF7 cells when compared to MDA-MB-231 cells with IC_{50} values being 53.55 µM and 58.62 µM respectively. Further testing of these compounds in HEK-293 cells did not display any toxicity (IC_{50}> 100 µM, **Table 1**) in normal cells, thus, making these compounds attractive for further derivatization and testing. The remaining compounds of the series displayed no activity against both breast cancer cell lines with IC_{50} values greater than 100 µM. Furthermore, all compounds showed no toxicity (IC_{50}> 100 µM) against A549 cells, and thus suggested their specificity towards the breast carcinoma cells.

10.1002/cbdv.201900462

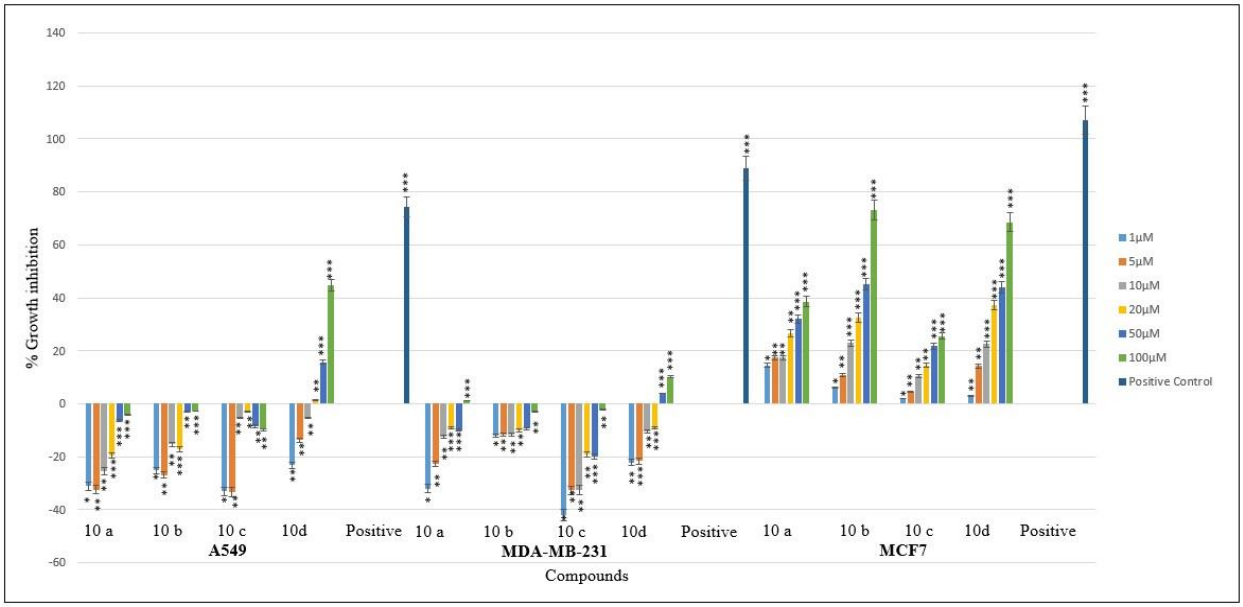

Figure 3. Representative graph comparing the percentage growth inhibition of A549, MCF**7** and MDA-MB-231 cells at selected concentrations of test compounds **10a**, **10b**, **10c** and **10d**. 40 µM Plumbagin was used as a positive control. Data are mean ± standard deviation S.D. (n=3), where *p<0.05, **p<0.01 and ***p<0.001 significant difference to untreated control.

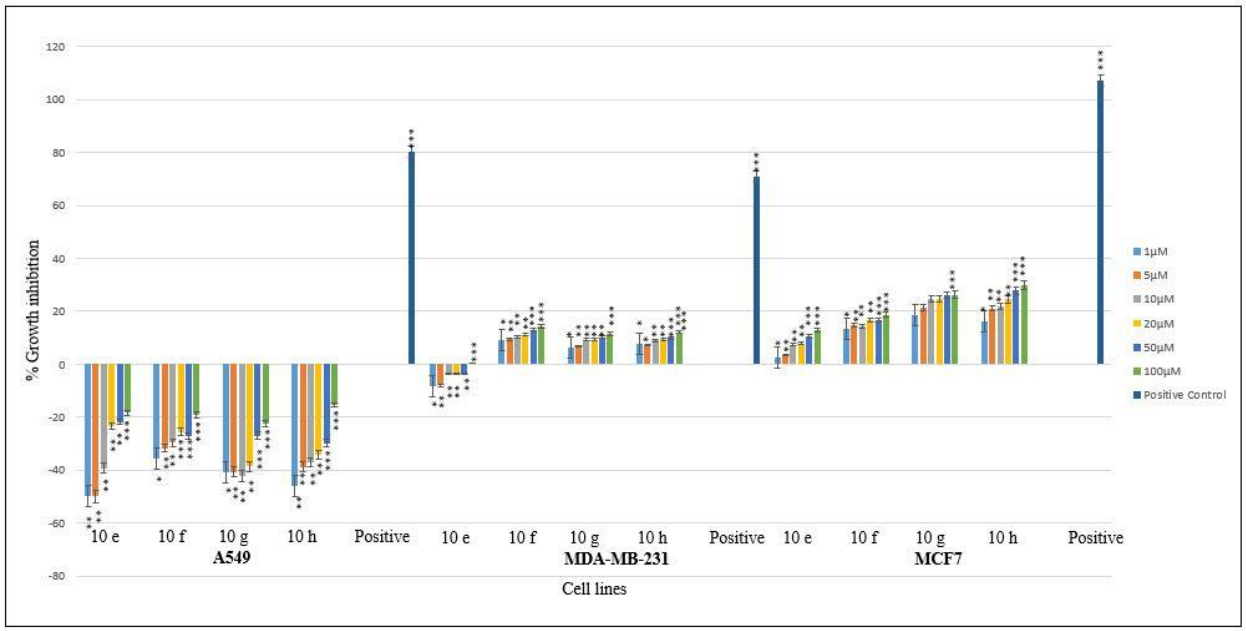

Figure 4. Representative graph comparing the percentage growth inhibition of A549, MCF**7** and MDA-MB-231 cells at selected concentrations of test compounds **10e**, **10f**, **10g** and **10h**. 40 µM Plumbagin was used as a positive control. Data are mean ± standard deviation S.D. (n=3), where *p<0.05, **p<0.01 and ***p<0.001 significant difference to untreated control.

10.1002/cbdv.201900462

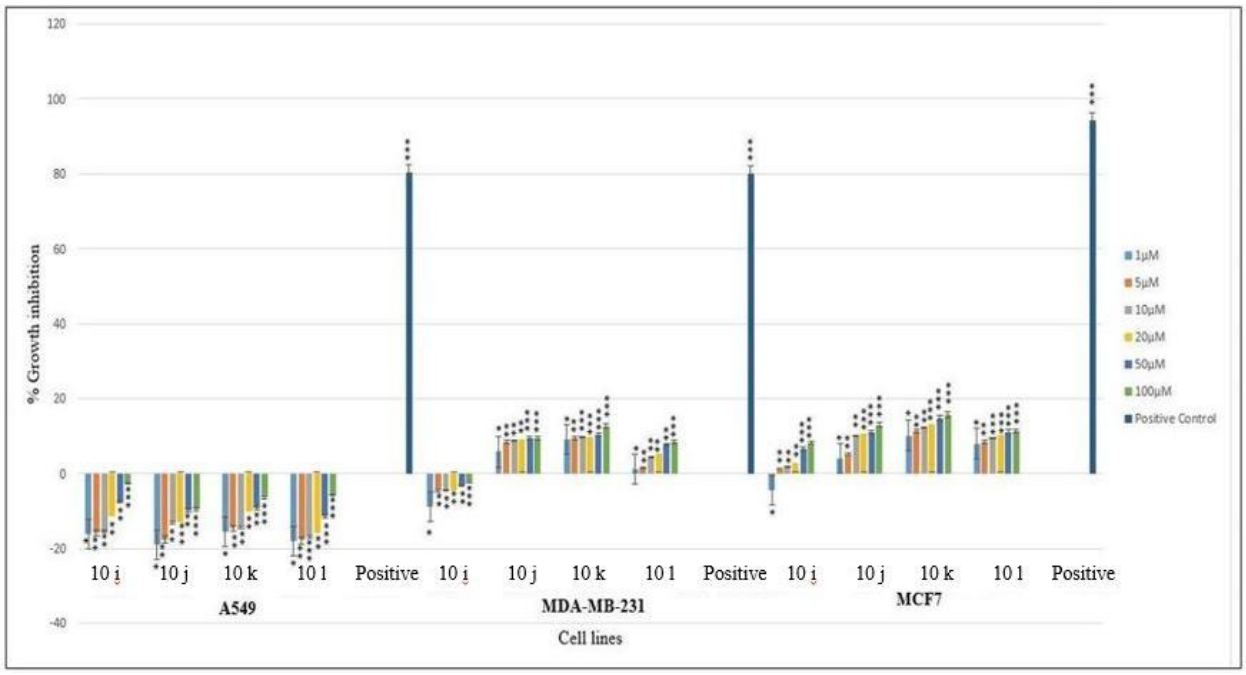

Figure 5. Representative graph comparing the percentage growth inhibition of A549, MCF**7** and MDA-MB-231 cells at selected concentrations of test compounds **10i**, **10j**, **10k** and **10l**. 40 µM Plumbagin was used as a positive control. Data are mean ± standard deviation S.D. (n=3), where *p<0.05, **p<0.01 and ***p<0.001 significant difference to untreated control.

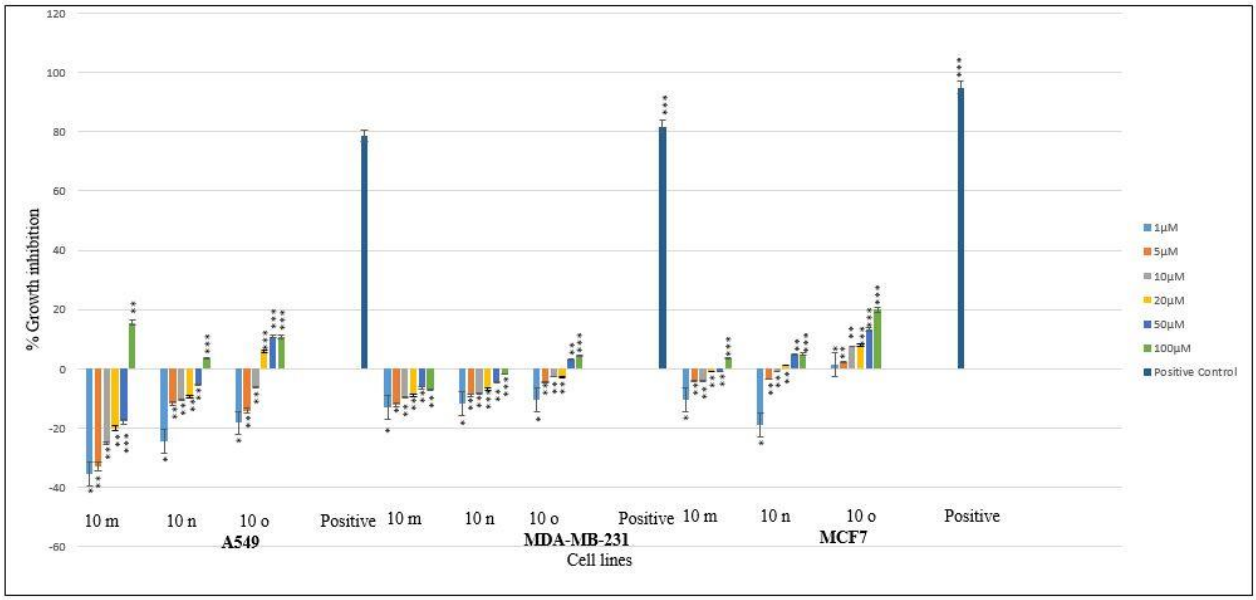

Figure 6. Representative graph comparing the percentage growth inhibition of A549, MCF7 and MDA-MB-231 cells at selected concentrations of test compounds **10m**, **10n** and **10o**. 40 µM

Plumbagin was used as a positive control. Data are mean ± standard deviation S.D. (n=3), where *p<0.05, **p<0.01 and ***p<0.001 significant difference to untreated control.

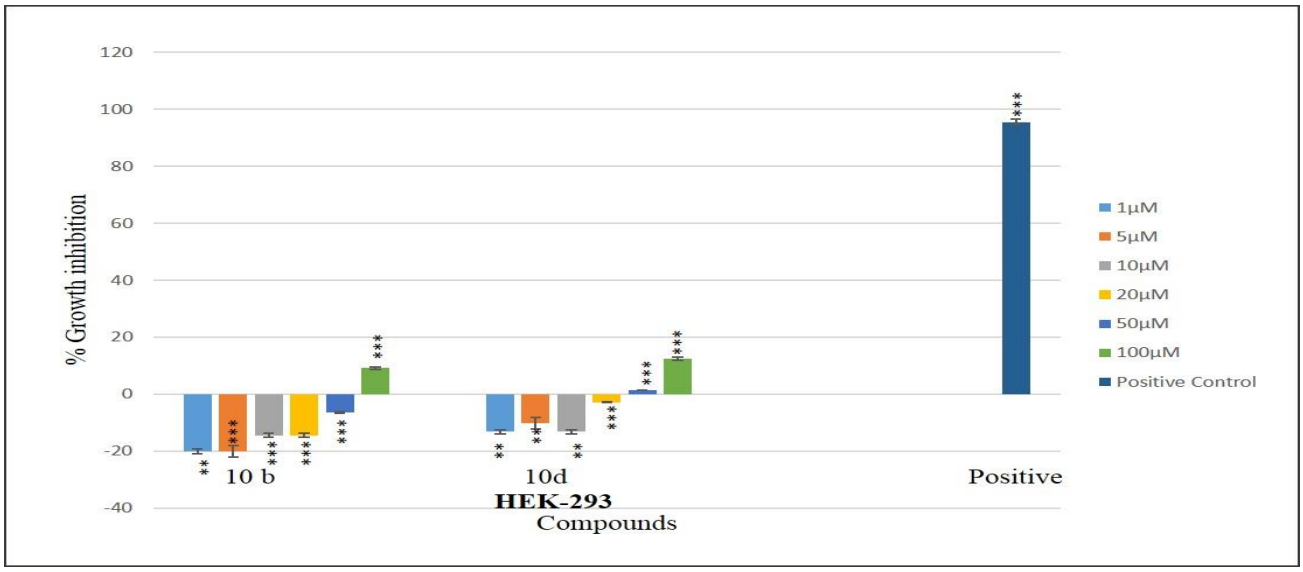

Figure 7. Representative graph comparing the percentage growth inhibition of HEK-293 cells at selected concentrations of test compounds **10b** and **10d**. 40 µM Plumbagin was used as a positive control. Data are mean ± standard deviation S.D. (n=3), where *p<0.05, **p<0.01 and ***p<0.001 significant difference to untreated control.

Structure-activity relationship (SAR) studies of the synthesized hybrids exhibited the dependency of activity on the type of phenyl rings substitutions present on N-1 of the β-lactam ring attached directly to triazole nucleus (**Fig. 8**). For instance, the *meta*-positioning of nitro (compound **10b**) and chloro (compound **10d**) group increased both the potency (IC_{50}<59 µM) and selectivity of these conjugates against MCF7 cancer cell line. However, their structural analogues (**10m** and **10l)** bearing mono-methylated coumarin ring were found to be inactive (IC_{50}>100 µM) against all the tested cell lines. The unsubstituted phenyl conjugates (**10a** and **10h**) also showed no cytotoxicity (IC_{50}>100 µM) against MDA-MB-231 and MCF7 cell lines. A summary of the result from the SAR study is presented in **Fig.8** below.

10.1002/cbdv.201900462

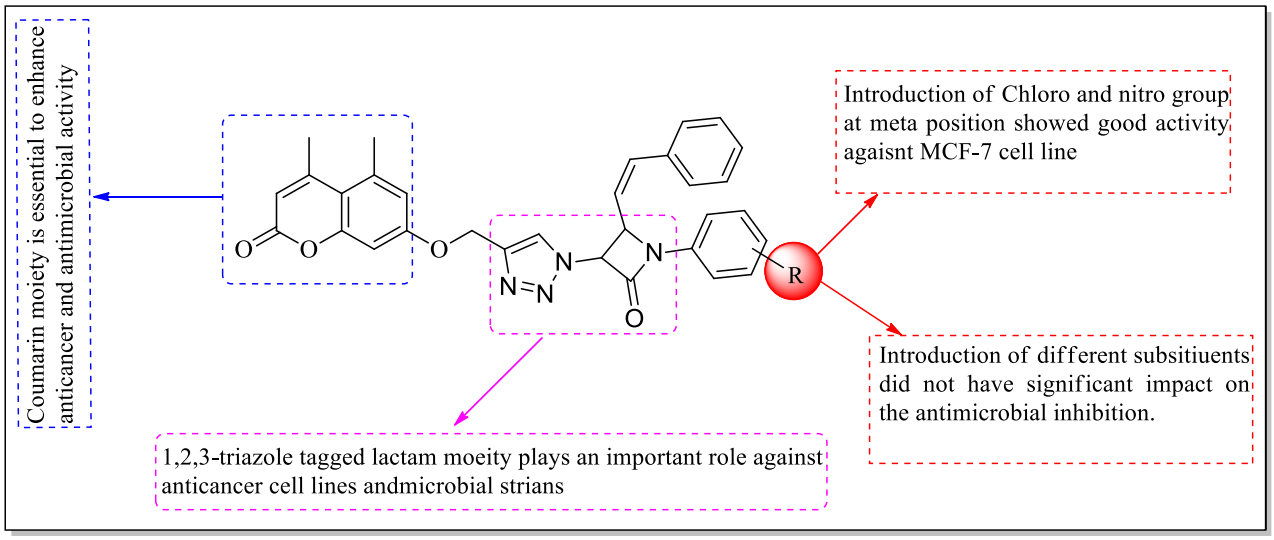

Figure 8. SAR study of phenyl substituted coumarin tagged 1,2,3-triazole with β-lactams as an anti-cancer agent and antimicrobial agent.

Analyzing the outcomes in **Table 1**, we could illustrate some suitable conclusions: 1) introduction of the nitro and chloro groups at *meta* position of the phenyl ring leads to anti-cancer activity of compounds (**10b** and **10d**) against MCF7 cells; 2) Conversely, there was a potency loss in compound **10l** and **10m** (IC_{50} >100 µM), where similar groups attached to the phenyl ring were introduced to the 4-methyl coumarin moiety, and 3) the positioning of electron-withdrawing groups (EWG) at position-3 of phenyl moiety generally offered more potent compounds against MCF7 cell-line.

10.1002/cbdv.201900462

Table 1: IC_{50} values of the synthesised compounds (**10a-g**/**10h-o**) againstA549 MCF7, MDA-MB-231 and HEK-293lines.

Code	Structure	A549 (µM)	MCF-7 (µM)	MDA-MB-231 cells (µM)	HEK-293 (µM)
10a	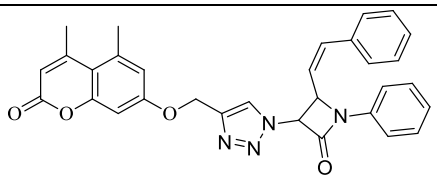	>100	>100	>100	-
10b	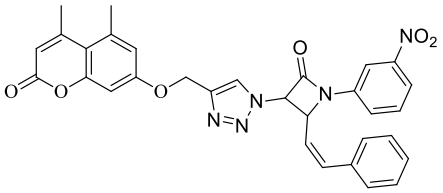	>100	**53.55**	>100	>100
10c	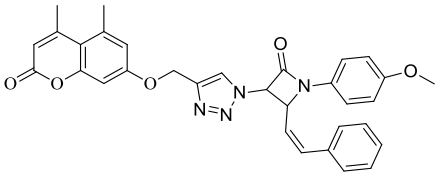	>100	>100	>100	-
10d	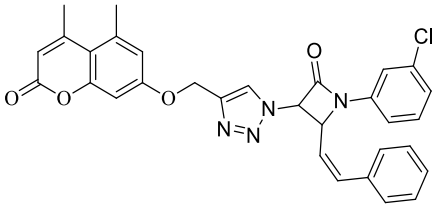	>100	**58.62**	>100	>100
10e	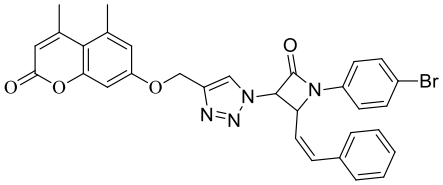	>100	>100	>100	-
10f	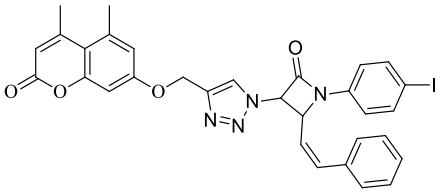	>100	>100	>100	-
10g	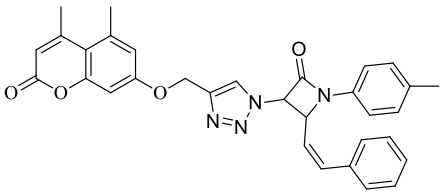	>100	>100	>100	-

10.1002/cbdv.201900462

10h	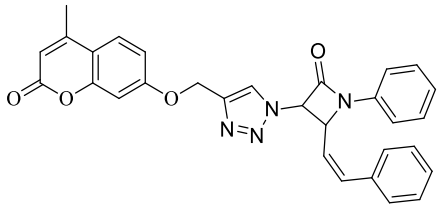	>100	>100	>100	-
10i	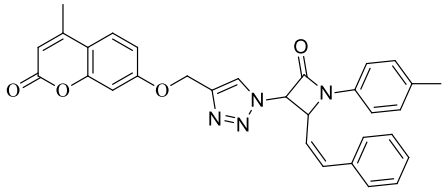	>100	>100	>100	-
10j	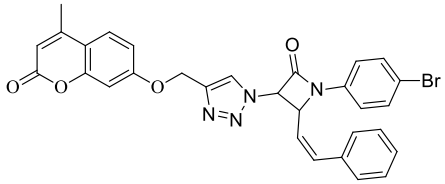	>100	>100	>100	-
10k	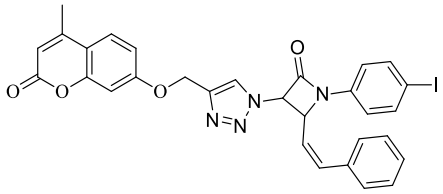	>100	>100	>100	-
10l	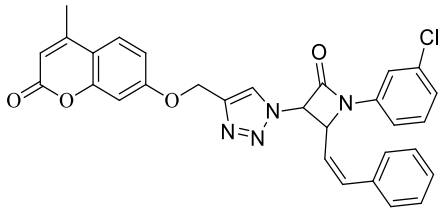	>100	>100	>100	-
10m	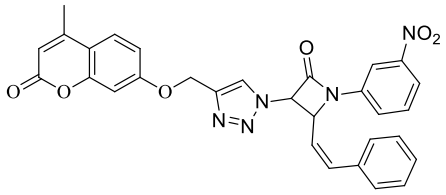	>100	>100	>100	-
10n	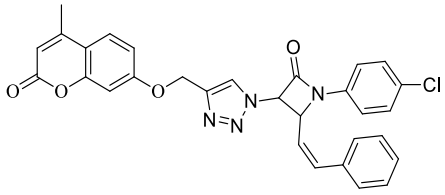	>100	>100	>100	-
10o	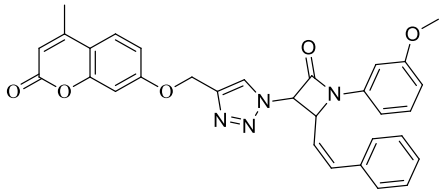	>100	>100	>100	-

Standard	**Plumbagin**	**11.69**	**3.5**	**4.4**	**NA**

Docking studies

The designed series of potential anti-breast cancer agents comprised 15 molecules with two distinct scaffolds; i.*e.***10b** and **10d**. The biological evaluation of the series refined the screen to identify a novel bioactive molecular hybrid encompassing critical pharmacophoric features which include a β-lactam, a dimethylated coumarin moiety, a 1,2,3-triazole and a phenyl ring with a C-3 substitution by a strongly electron-withdrawing group. These characteristics were most prominent and conserved between the most active inhibitors **10b** and **10d**. It was also unique to find that these potential drug candidates selectively inhibited the MCF7 cell-line, which emphasizes the affinity of the designed conjugate to target estrogen receptor-α (ER-α). Molecular docking of the most active ligands in ER-α was performed to understand the binding interactions critical to induce a pharmacological response.

Table 2: Docking scores of ligands in the binding pocket of ER-α

Ligand Identifier	Docking score/ (kcal/mol)	RMSD i.b.	RMSD u.b.
10a	-10.9	0.000	0.000
10b	-11.3	0.000	0.000
10c	-10.7	0.000	0.000
10d	-10.9	0.000	0.000

10.1002/cbdv.201900462

10e	-11.0	0.000	0.000
10f	-11.3	0.000	0.000
10g	-11.0	1.906	3.708
10h	-10.4	1.719	2.542
10i	-10.7	0.000	0.000
10j	-10.5	0.000	0.000
10k	-10.6	0.000	0.000
10l	-10.4	2.116	3.747
10m	-10.3	1.611	2.615
10n	-10.7	0.000	0.000
10o	-9.7	1.740	2.474

Compound **10b** exhibited an extensive interaction with the binding domain of the receptor (docking score = -11.3 kcal/mol, (**Table 2**) and was more potent than compound **10d** (IC_{50} = 53.55 and 58.62 μM respectively). The interaction profile was primarily governed by Vander Waals and hydrophobic interactions between residues Leu41, Ala45, Leu49, Trp78, Phe99, Ile119, Leu123, Lys224, Val228 and Leu231 with the carbons of the coumarin ring, nitro-substituted phenyl ring and methylene linked phenyl ring (bond distance = 3.92, 3.89, 3.71, 3.80, 3.66, 3.65, 3.94, 3.31, 3.26 and 3.93 Å, respectively). This was accompanied by two well-defined hydrogen bonds between the protein donor residues Thr42 and Leu231 with the nitrogen of the triazole group and the oxygen of the nitro moiety (bond distance = 3.99 and 2.96 Å; bond angle = 176.64˚ and 138.38˚, respectively). As mentioned earlier, the presence of an electron withdrawing group,*i.e.* a nitro group for compound **10b**, at the C-3 position of the *N*-linked phenyl group has a direct impact on

the potency of the inhibitor. This is attributed to the formation of a unique electrostatic interaction, a T-shaped π-stacking between residue Trp78 and the methylene linked phenyl ring (distance = 4.71 Å, angle = 63.45˚).

The interaction network of compound **10d** is also grounded by multiple hydrophobic interactions between receptor residue Leu41, Ala45, Leu86, Leu123, Val228, Leu231 and Leu234 with the phenyl and coumarin rings of the ligand (bond distance = 3.72, 3.74, 3.49, 3.91, 3.49, 3.85 and 3.43 Å, respectively). The differences in **10d** and **10b** binding landscapes are first observed with the single hydrogen bond formation in the complex of **10d** between amino acid Thr42 and the nitrogen of the triazole (bond distance = 3.24 Å and bond angle = 137.56˚). The lack of the additional stabilizing hydrogen bond could possibly be a reason for the slight discrepancy in the efficacy of compound **10d** (IC_{50} value ~53.62 μM less than compound **10b**). However, the ligand appears to compensate for the loss of the feature by forming a salt bridge to facilitate charge transfer between residue Arg89 and the carboxylate of the coumarin ring at a bond distance of 5.38 Å. The electron-withdrawing group of compound **10d** is a chlorine atom which when bound in the catalytic domain of the receptor forms an electrostatic interaction with amino acid Val229 at a distance of 3.22 Å (donor angle = 145.82˚ and acceptor angle = 126.15˚).

From **Table 3** it is evident that the presence of the nitro group in compound **10b** significantly alters the lipophilicity of the inhibitor, whereby the more lipophilic the molecule, the more potent the potential drug is against the MCF7 cell line. The total polar surface area of compound **10b** is greater than compound **10d,** which may be a contributing feature to a more potent anti-breast cancer agent. The inhibitory activity also appears to be affected by the ligands ability to form hydrogen bond in the active site, thus greater number of acceptor pharmacophores will result in an improved inhibitory effect.

10.1002/cbdv.201900462

The results observed from docking highlight the advantageous utilization of the coumarin-triazole-β-lactam molecular hybrid in the future design and development of novel and efficient anti-breast cancer chemotherapeutics.

Table 3: Physical properties of the most active compounds against MCF7 cell-line

Compound ID	clog P	TPSA / Å^2	Rotatable bonds	Molecular Weight/ g.mol^{-1}	Pharmacophore features		
					Acceptors	Donors	Ionisable groups/charge
10b	3.89	136.28	8	563.56	8	0	1/-
10d	4.96	90.46	7	553.01	6	0	1/-

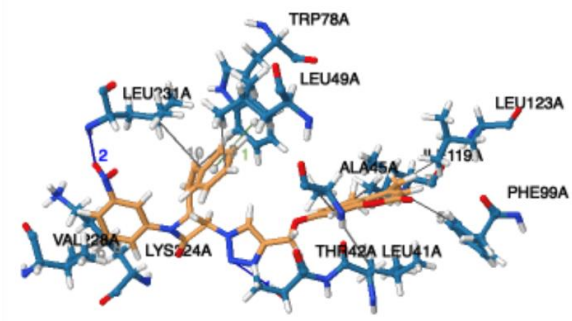

Compound **10b**

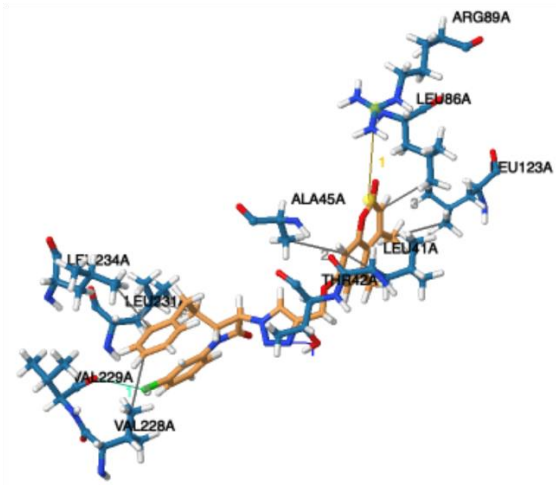

Compound **10d**

Figure 9: Three-dimensional structure of compounds **10b** and **10d** in complex with ER-α.

Antimicrobial Evaluation

In this study, five bacterial strains *viz*; a Gram-positive Methicillin-resistant *Staphylococcus aureus* (MRSA; ATCC 43300) and four Gram-negative bacteria (*Pseudomonas aeruginosa* ATCC 27853, *Klebsiella pneumonia* ATCC 700603, *Escherichia coli* ATCC 25922, and *Acinetobacter baumannii* ATCC 19606) and two fungal strains (*Candida albicans* ATCC 90028, and *Cryptococcus neoformans* H99; ATCC 208821) were used to determine the antimicrobial activity of the synthesized compounds. The disc diffusion method was only used to detect the antibacterial activity of the test compounds at a concentration of 32 µg mL^{-1} with ≤1% DMSO. The results showed that the test compounds were moderately active against MRSA, *Klebsiella pneumonia, Pseudomonas aeruginosa, Acinetobacter baumannii* bacterial strains, and *Candida albicans* fungal strain. Further, out of this, only three of the test compounds, the **10c**, **10f**, and **10g** compounds exhibited activity against MRSA while most of the test compounds showed moderate activity in the other strains (**Table 4**). However, the test compounds did not show any antibacterial activity against *Escherichia coli* whereas, compounds **10a**, **10d**, and **10e** were found to be inactive against *Pseudomonas aeruginosa*.

The three compounds that exhibited activity against MRSA, **10c**, **10f**, and **10g** had values that showed a maximum percentage inhibition 7.75, 7.92, and 8.94% respectively and other compounds were found to be inactive against these strains. Further, the test compound **10i**, **10j**, **10k**, and **10d** were found to be more active with percentage inhibition values of 21.65, 9.42, 6.24, and 14.96 against *Candida albicans* fungal strain (**Table 4**). However, all the test compounds were recorded inactive against *Cryptococcus neoformans.*

10.1002/cbdv.201900462

Table 4: Antibacterial and antifungal screening data of compounds **10a-g** and **10h-o**

Percentage inhibition (%) *							
	Bacterial Strain					**Fungal Strian**	
Compound Name	Sa	Ec	Kp	Pa	Ab	Ca	Cn
10a	-	-	-	-	-	-	-
10b	-	-	-	10.44	-	16.18	-
10c	7.75	-	-	18.97	-	-	-
10d	-	-	-	-	-	14.96	-
10e	-	-	-	-	-	4.35	-
10f	7.92	-	6.91	17.78	7.8		-
10g	8.94	-	4.87	11.11	0.22	4.29	-
10h	-	-	2.33	12.11	-	2.6	-
10i	-	-	-	4.39	-	21.65	-
10j	-	-	-	5.74	-	9.42	-
10k	-	-	3.41	7.32	-	6.24	-

10.1002/cbdv.201900462

10l	-	-	0.05	16.37	-	3.0	-
10m	-	-	-	7.74	-	-	-
10n	-	-	-	6.66	-	-	-
10o	-	-	2.74	8.47	2.29	3.47	-

* All percentage inhibitions were determined at 32 µg/mL.Sa = *Staphylococcus aureus,* Ec = *Escherichia coli*, Kp = *Klebsiella pneumonia,* Pa = *Pseudomonas aeruginosa,* Ab = *Acinetobacterbaumannii,* Ca = *Candida albicans,* Cn = *Cryptococcus neoformans*; DMSO, negative control; Colistin and Vancomycin were used as standards for antibacterial activity while Fluconazole was used as standard for antifungal activity.

All the tested compounds were found to be less active than they used standard drugs (Colistin and Vancomycin for bacterial and Fluconazole for fungal strains).

Conclusions

Novel coumarin-β-lactam-triazole molecular hybrids were synthesized using the copper(I)-catalyzed Huisgen 1,3-dipolar cycloaddition reaction. The biological evaluation of these compounds three cancer cell lines (MDA-MB-231, MCF7, A549) and one control cell line HEK-293 revealed two potent compounds (**10b** and **10d**)against MCF-7 cancer cells with no toxicity against the normal cells. Further, the antimicrobial studies concluded that the compounds bearing iodo and methyl groups displayed moderate antimicrobial activity against *Pseudomonas aeruginosa* and *Candida albicans* strains. Thus, further modification and structure derivatization of these compounds may result in the introduction of selective anti-breast cancer agents.

Experimental section

Chemistry

The progress of all reactions was monitored by pre-coated *Merck* silica gel 60F-254 TLC plates, using 254 nm UV light for visualisation. ^{1}H NMR and ^{13}C NMR spectra were on Bruker 400 and 600 MHz NMR spectrometer. Chemical shifts given in δ values (ppm) using tetramethylsilane as internal standard referenced to the residual solvents signal of $CDCl_3$ at δ 7.26 ppm for ^{1}H and δ 77.39 ppm for ^{13}C and residual signal for DMSO at δ 2.50 ppm for ^{1}H and δ 39.50 ppm for ^{13}C. Chemical shift values expressed in parts per million (ppm) downfield from TMS and J values in Hertz. Splitting patterns indicated as s: singlet, d: doublet, t: triplet, m: multiplet, dd: double doublet, and br: broad peak. Resonance assigned by chemical shift, a multiplicity of resonance, signal intensities and H-H coupling constants. Mass spectra were recorded using high-resolution mass spectrometer (HRMS). The IR spectra recorded on an FTIR spectrophotometer. Chromatographic separations were carried out on 60:120 silica gel using EtOAc and hexane mixture as eluent.

General Procedure for the synthesis of 7-hydroxy-4,5-dimethyl coumarin **(8a)** and *7-hydroxy-4-methyl-2H-chromen-2-one* (**8b**)

In two different 50 mL round-bottom flasks, equimolar quantities of 5-methylbenzene-1,3-diol (**7a**) (1.0 eq), ethyl acetoacetate (1.0 eq) for the synthesis of compound **8a** and 3-hydroxy phenol (**7b**) (1.0 eq), ethyl acetoacetate (1.0 eq) for compound **8b,** were added to stirring concentrated sulfuric (H_2SO_4) at 0-5°C and stirred for 2.0 hrs. The reactions were monitored by the TLC. After reaction completion, the reaction mixtures were poured into the crushed ice with continuous stirring and then filtered, washed with water and recrystallised with ethanol to get **7**-hydroxy-4,5-dimethyl-2H-chromen-2-one (**8a**) and 7-hydroxy-4-methyl-2H-chromen-2-one (**8b**). The pure products were obtained in **83-85%** yield. m.p. Found: 260-262°C (**8a**) and 186-188°C (**8b**).

General procedure for the synthesis of procedure for the preparation of β-lactam Coumarin conjugates **(*10a-g*** and ***10h-o*)**

To a stirred solution of **7**-(ethynyloxy)-4,5-dimethyl-2H-chromen-2-one (**9a)** and 4-methyl-**7**-(prop-2-yn-1-yloxy)-2H-chromen-2-one (**9b)** (1 mmol for **9a** and **9b**) in DCM:H_2O (8:2), theazidoβ-lactam(**6a-h)** (2 mmol for **9a** and **9b**) was added, followed by the addition of copper sulphate (0.055 mmol for **9a** and **9b**) and sodium ascorbate (0.13 mmol for **9a** and **9b**) at room temperature. The progress of the reaction was monitored using TLCuntil the disappearance of starting material was observed then, and water was added (15 mL) to the reaction mixture and extracted with chloroform (50 mL). Combined organic layers was dried with anhydrous sodium sulfate and concentrated under reduced pressure to result in the isolation of a crude productwhich was purified by silica gel chromatography using 4:6 (EtOAc:hexane) for (**10a-g)** and **(10h-o)** compounds.

*(Z)-3-(4-(((4,5-dimethyl-2-oxo-2H-chromen-**7**-yl)oxy)methyl)-1H-1,2,3-triazol-1-yl)-1-phenyl-4-styrylazetidin-2-one* (***10a***)

Yield-76%; mp 213-215 ^{0}C; Cream amorphous solid; IR (neat) (ν_{max}/cm^{-1}): 2933, 1755, 1713, 1600; ^{1}H NMR (400 MHz, $CDCl_3$) δ 7.84 (s, 1H, triazole-CH), 7.54 (d, *J* = 7.9 Hz, 2H, ArH), 7.38 (t, *J* = 7.8 Hz, 2H. ArH), 7.28 (s, 1H, ArH), 7.21 (dd, *J* = 16.6, 7.3 Hz, 4H, ArH), 7.14 (d, *J* = 6.3 Hz, 2H, ArH), 6.77 (d, *J* = 16.0 Hz, 1H, Vinyl-CH), 6.73 (s, 1H, Coumarin-CH), 6.64 (s, 1H, Coumarin-CH), 6.27 (d, *J* = 5.4 Hz, 1H, Vinyl-CH), 5.90 (dd, *J* = 14.8, 8.5 Hz, 1H, lactam-CH), 5.27 – 5.24 (m, 1H, lactam-CH), 5.18 (s, 2H, CH_2), 2.33 (s, 3H, CH_3), 2.17 (s, 3H, CH_3). ^{13}C NMR (101 MHz, $CDCl_3$) δ 160.84, 158.53, 156.23, 155.20, 153.91, 143.06, 143.17, 137.80, 136.84, 134.79, 129.45, 129.00, 128.73, 126.70, 125.48, 123.64, 119.69, 117.44, 113.60, 110.86, 108.40,

108.32, 67.19, 62.18, 60.06, 24.15, 21.93. HRMS of $[C_{31}H_{26}N_4O_4 + Na]^+$ (m/z): 541.1852; Calcd: 541.1850.

*(Z)-3-(4-(((4,5-dimethyl-2-oxo-2H-chromen-**7**-yl)oxy)methyl)-1H-1,2,3-triazol-1-yl)-1-(3-nitrophenyl)-4-styrylazetidin-2-one* (***10b***)

Yield-80%; mp 188-190 ^{0}C; Yellow amorphous solid; IR (neat) (ν_{max}/cm^{-1}): 1755, 1603, 1488;^{1}H NMR (400 MHz, $CDCl_3$) δ 7.85 (s, 1H, triazole-CH), 7.53 (d, *J* = 7.6 Hz, 2H, ArH), 7.37 (t, *J* = 7.4 Hz, 2H, ArH), 7.20 (dd, *J* = 16.6, 7.1 Hz, 4H, ArH), 7.13 (s, 2H, ArH), 6.80 – 6.67 (m, 2H, ArH), 6.62 (s, 1H, Coumarin-CH), 6.26 (d, *J* = 4.9 Hz, 1H, Vinyl-CH), 5.89 (t, *J* = 11.4 Hz, 2H, lactam-CH), 5.27 (d, *J* = 6.0 Hz, 1H, lactam-CH), 5.19 (s, 2H, CH_2), 2.33 (s, 3H, CH_3), 2.17 (s, 3H, CH_3). ^{13}C NMR (101 MHz, $CDCl_3$) δ 160.86, 158.55, 156.23, 155.18, 153.94, 143.07, 137.80,136.84, 134.79, 129.45, 129.00, 128.73, 126.70, 125.47, 123.66, 119.71, 117.43, 113.58, 110.85, 108.39, 108.32, 77.37, 77.05, 76.73, 67.19, 62.18, 60.07, 24.15, 21.93. HRMS of $[C_{31}H_{25}N_5O_6 + Na]^+$(m/z): 586.1703; Calcd: 586.1796.

*(Z)-3-(4-(((4,5-dimethyl-2-oxo-2H-chromen-**7**-yl)oxy)methyl)-1H-1,2,3-triazol-1-yl)-1-(3-methoxyphenyl)-4-styrylazetidin-2-one* (***10c***)

Yield-83%; mp 198-200 ^{0}C; White amorphous solid; IR (neat) (ν_{max}/cm^{-1}): 1715, 1606, 1488;^{1}H NMR (400 MHz, $CDCl_3$) δ 7.84 (s, 1H, triazole-CH), 7.58 – 7.40 (m, 2H, ArH), 7.27 – 7.20 (m, 3H, ArH), 7.13 (dd, *J* = 7.7, 1.6 Hz, 2H, ArH), 6.94 – 6.89 (m, 2H, ArH), 6.76 (d, *J* = 3.2 Hz, 1H, Vinyl-CH), 6.73 (s, 1H, Coumarin-CH), 6.65 (s, 1H, Coumarin-CH), 6.25 (d, *J* = 5.4 Hz, 1H, Vinyl-CH), 5.93 (d, *J* = 0.9 Hz, 1H, Coumarin-CH), 5.87 (dd, *J* = 16.0, 7.3 Hz, 1H, lactam-CH), 5.26 – 5.22 (m, 1H, lactam-CH), 5.22 (s, 2H, CH_2), 3.81 (s, 3H,Ar-OCH_3), 2.36 (s, 3H, CH_3), 2.21 (d, *J* = 0.9 Hz, 3H, CH_3). ^{13}C NMR (101 MHz, $CDCl_3$) δ 160.84, 157.91, 157.13, 156.24, 155.20, 153.90, 143.05, 137.73, 134.80, 130.26, 128.98, 128.73, 126.68, 123.59, 119.82, 118.85, 114.61,

113.61, 110.87, 108.32, 67.22, 62.19, 60.11, 55.51, 24.16, 21.94. HRMS of $[C_{32}H_{28}N_4O_5 + Na]^+$(m/z): 571.1957; Calcd: 571.1953.

*(Z)-1-(3-chlorophenyl)-3-(4-(((4,5-dimethyl-2-oxo-2H-chromen-**7**-yl)oxy)methyl)-1H-1,2,3-triazol-1-yl)-4-styrylazetidin-2-one* (***10d***)

Yield-86%; mp 188-190 ^{0}C; Cream amorphous solid; IR (neat) (ν_{max}/cm^{-1}): 1714, 1608, 1383; ^{1}H NMR (400 MHz, $CDCl_3$) δ 7.83 (s, 1H, triazole-CH), 7.47 (d, *J* = 8.6 Hz, 2H, ArH), 7.33 (d, *J* = 8.6 Hz, 2H, ArH), 7.23 (d, *J* = 6.9 Hz, 3H, ArH), 7.13 (d, *J* = 6.7 Hz, 2H, ArH), 6.79 – 6.70 (m, 2H, ArH), 6.62 (s, 1H, Coumarin-CH), 6.26 (d, *J* = 5.4 Hz, 1H, Vinyl-CH), 5.87 (dd, *J* = 16.4, 6.8Hz, 2H, lactam-CH), 5.26 – 5.21 (m, 1H, lactam-CH), 5.19 (s, 2H, CH_2), 2.33 (s, 3H, CH_3), 2.17 (s, 3H, CH_3). ^{13}C NMR (101 MHz, $CDCl_3$) δ 160.83, 158.43, 156.19, 155.19, 153.87, 143.08, 138.13, 135.32, 134.60, 130.69, 129.57, 129.16, 128.78, 126.72, 119.26, 118.67, 113.61, 110.89, 108.39, 108.32, 67.38, 62.17, 60.28, 24.15, 21.93. HRMS of $[C_{31}H_{25}ClN_4NaO_4 + Na]^+$ (m/z): 575.1462; Calcd: 575.1448.

*(Z)-1-(4-bromophenyl)-3-(4-(((4,5-dimethyl-2-oxo-2H-chromen-**7**-yl)oxy)methyl)-1H-1,2,3-triazol-1-yl)-4-styrylazetidin-2-one* (***10e***)

Yield-78%; mp 217-219 ^{0}C; Cream amorphous solid; IR (neat) (ν_{max}/cm^{-1}): 1756, 1716, 1605, 1488;^{1}H NMR (400 MHz, $CDCl_3$) δ 7.82 (s, 1H, triazole-CH), 7.44 (dd, *J* = 27.3, 8.7 Hz, 4H, ArH), 7.28 – 7.18 (m, 3H, ArH), 7.13 (d, *J* = 6.7 Hz, 2H, ArH), 6.77 (s, 1H, Coumarin-CH), 6.72 (d, *J* = 3.8 Hz, 2H, Vinyl-CH)., 6.62 (s, 1H, Coumarin-CH), 6.25 (d, *J* = 5.4 Hz, 1H, Vinyl-CH), 5.87 (dd, *J* = 16.3, 7.1 Hz, 1H, lactam-CH), 5.27 – 5.21 (m, 1H, lactam-CH), 5.19 (s, 2H, CH_2), 2.33 (s, 3H, CH_3), 2.17 (s, 3H, CH_3). ^{13}C NMR (101 MHz, $CDCl_3$) δ 160.82, 158.49, 156.20, 155.19, 153.87, 143.07, 138.14, 135.79, 134.60, 132.49, 129.16, 128.78, 126.72, 123.64, 119.24,

118.97, 118.33, 113.61, 110.88, 108.38, 108.32, 67.38, 62.17, 60.26, 24.15, 21.94. HRMS of $[C_{31}H_{25}BrN_4O_4 + Na]^+$ (m/z): 619.0957; Calcd: 619.0952.

*(Z)-3-(4-(((4,5-dimethyl-2-oxo-2H-chromen-**7**-yl)oxy)methyl)-1H-1,2,3-triazol-1-yl)-1-(4 iodophenyl)-4-styrylazetidin-2-one* (***10f***)

Yield-87%; mp 212-214 ^{0}C; White amorphous solid; IR (neat) (ν_{max}/cm^{-1}): 1757, 1717, 1605, 1487;^{1}H NMR (400 MHz, $CDCl_3$) δ 7.83 (s, 1H, triaozle-CH), 7.67 (d, *J* = 8.3 Hz, 2H, ArH), 7.35 – 7.18 (m, 5H, ArH), 7.12 (d, *J* = 6.5 Hz, 2H, ArH), 6.74 (d, *J* = 16.9 Hz, 2H, Vinyl-CH), 6.62 (s,1H, Coumarin-CH), 6.25 (d, *J* = 5.2 Hz, 1H, Vinyl-CH), 5.92 – 5.82 (m, 2H, lactam CH, Coumarin-CH), 5.26 – 5.21 (m, 1H, lactam-CH), 5.19 (s, 2H, CH_2), 2.33 (s, 3H, CH_3), 2.17 (s, 3H, CH_3). ^{13}C NMR (101 MHz, $CDCl_3$) δ 160.81, 158.53, 156.20, 155.20, 153.85, 143.26, 143.06, 138.40, 138.11, 136.41, 134.60, 129.15, 128.78, 126.72, 123.61, 119.21, 113.62, 110.89, 108.31, 89.06, 67.37, 62.17, 60.18, 24.15, 21.94. HRMS of $[C_{31}H_{25}IN_4NaO_4 + Na]^+$ (m/z): 667.0818; Calcd: 667.0809.

*(Z)-3-(4-(((4,5-dimethyl-2-oxo-2H-chromen-**7**-yl)oxy)methyl)-1H-1,2,3-triazol-1-yl)-4-styryl-1-(p-tolyl)azetidin-2-one (**10g**)*

Yield-81%; mp 220-222 ^{0}C; White amorphous solid; IR (neat) (ν_{max}/cm^{-1}): 1753, 1713, 1610, 1492; ^{1}H NMR (400 MHz, $CDCl_3$) δ 7.84 (s, 1H, triazole-CH), 7.41 (d, *J* = 8.3 Hz, 2H, ArH), 7.25 – 7.06 (m, 7H, ArH), 6.76 (s, 1H, Coumarin-CH), 6.72 (s, 1H, Coumarin-CH), 6.62 (s, 1H, ArH), 6.24 (d, *J* = 5.4 Hz, 1H, Vinyl-CH), 5.86 (dd, *J* = 14.6, 5.8 Hz, 2H, lactam-CH), 5.25 – 5.20 (m, 1H, lactam-CH), 5.18 (s, 2H, CH_2), 2.33 (d, *J* = 3.2 Hz, 6H, 2 CH_3), 2.17 (s, 3H, Ar-CH_3). ^{13}C NMR (101 MHz, $CDCl_3$) δ 160.84, 158.26, 156.24, 155.19, 153.92, 143.13, 143.04, 137.65, 135.30, 134.84, 134.39, 129.91, 128.95, 128.71, 126.68, 123.62, 119.80, 117.38, 113.59, 110.84,

108.39, 108.31, 67.17, 62.18, 59.96, 24.15, 21.94, 21.01. HRMS of $[C_{32}H_{28}N_4NaO_4 + Na]^+$ (m/z): 555.2008; Calcd: 555.1995.

*(Z)-3-(4-(((4-methyl-2-oxo-2H-chromen-**7**-yl)oxy)methyl)-1H-1,2,3-triazol-1-yl)-1-phenyl-4-styrylazetidin-2-one* (***10h***)

Yield-78%; mp 172-174 ^{0}C; Brown amorphous solid; IR (neat) (ν_{max}/cm^{-1}): 1759, 1709, 1611, 1387; ^{1}H NMR (400 MHz, $CDCl_3$) δ 7.87 (s, 1H, triazole-CH), 7.52 (d, *J* = 7.8 Hz, 2H, ArH),7.44 – 7.32 (m, 3H, ArH), 7.24 – 7.14 (m, 4H, ArH), 7.11 (dd, *J* = 6.6, 2.8 Hz, 2H, ArH), 6.87 – 6.79 (m, 2H, Coumarin-CH), 6.75 (d, *J* = 16.0 Hz, 1H, Vinyl-CH), 6.25 (d, *J* = 5.4 Hz, 1H, Vinyl-CH), 6.12 (s, 1H, Coumarin-CH), 5.86 (dd, *J* = 16.0, 7.4 Hz, 1H, lactam-CH), δ 5.25 (dd, *J* = 14.4, 8.1 Hz, 1H, lactam-CH), 5.20 (s, 2H, CH_2), 2.36 (s, 3H, CH_3). ^{13}C NMR (101 MHz, $CDCl_3$) δ 161.16, 160.99, 158.53, 155.05, 152.43, 143.44, 137.80, 136.87, 134.89, 129.42, 128.85, 128.65, 126.75, 125.66, 125.42, 123.70, 119.82, 117.44, 114.07, 112.29, 112.15, 102.12, 67.26, 62.04, 60.02, 18.65. HRMS of $[C_{30}H_{24}N_4O_4 + Na]^+$ (m/z): 527.1695; Calcd: 527.1680.

*(Z)-3-(4-(((4-methyl-2-oxo-2H-chromen-**7**-yl)oxy)methyl)-1H-1,2,3-triazol-1-yl)-4-styryl-1-(p-tolyl)azetidin-2-one* (***10i***)

Yield-76%; mp 198-200 ^{0}C; White amorphous solid; IR (neat) (ν_{max}/cm^{-1}): 1757, 1711, 1610, 1387; ^{1}H NMR (400 MHz, $CDCl_3$) δ 7.86 (s, 1H, triazole-CH), 7.43 – 7.38 (m, 3H, ArH), 7.22 – 7.19 (m, 3H, ArH), 7.16 (d, *J* = 8.1 Hz, 2H, ArH), 7.11 (dd, *J* = 6.7, 2.9 Hz, 2H, ArH), 6.85 – 6.79 (m, 2H, Coumarin-CH), 6.73 (d, *J* = 16.0 Hz, 1H, Vinyl-CH), 6.23 (d, *J* = 5.4 Hz, 1H, Vinyl-CH), 6.13 (s, 1H, Coumarin-CH), 5.83 (dd, *J* = 16.0, 7.2 Hz, 1H, lactam-CH), 5.21 (dd, *J* = 4.0, 3.4 Hz, 1H, lactam-CH), 5.19 (s, 2H, CH_2), 2.37 (s, 3H, CH_3), 2.32 (s, 3H, CH_3). ^{13}C NMR (101 MHz, $CDCl_3$) δ 161.17, 161.00, 158.25, 155.05, 152.43, 143.39, 137.65, 135.24, 134.93, 134.42, 129.89,

128.80, 128.63, 126.73, 125.65, 123.69, 119.91, 117.38, 114.07, 112.29, 112.14, 102.13, 67.24, 62.04, 59.91, 21.00, 18.65. HRMS of $[C_{31}H_{26}N_4O_4 + Na]^+$ (m/z): 541.1852; Calcd: 541.1846.

*(Z)-1-(4-bromophenyl)-3-(4-(((4-methyl-2-oxo-2H-chromen-**7**-yl)oxy)methyl)-1H-1,2,3-triazol-1-yl)-4-styrylazetidin-2-one* (***10j***)

Yield-79%; mp 224-226 ^{0}C; Cream amorphous solid; IR (neat) (ν_{max}/cm^{-1}): 1758, 1710, 1611, 1386; ^{1}H NMR (400 MHz, $CDCl_3$) δ 7.85 (s, 1H, triazole-CH), 7.52 – 7.45 (m, 2H, ArH), 7.41 (dt, *J* = 5.3, 3.3 Hz, 3H, ArH), 7.22 (dd, *J* = 5.0, 1.8 Hz, 3H, ArH), 7.12 (dd, *J* = 6.5, 3.0 Hz, 2H, ArH), 6.83 (dd, *J* = 7.6, 2.2 Hz, 2H, Coumarin-CH), 6.74 (d, *J* = 16.0 Hz, 1H, Vinyl-CH), 6.25 (d, *J* = 5.5 Hz, 1H, Vinyl-CH), 6.13 (d, *J* = 1.1 Hz, 1H, Coumarin-CH), 5.84 (dd, *J* = 16.0, 7.5 Hz, 1H, lactam-CH), 5.24 – 5.21 (m, 1H, lactam-CH), 5.20 (s, 2H, CH_2), 2.37 (d, *J* = 1.0 Hz, 3H, CH_3). ^{13}C NMR (101 MHz, $CDCl_3$) δ 161.22, 160.96, 158.48, 152.49, 143.51, 138.14, 135.81, 134.68, 132.47, 129.01, 128.70, 126.77, 125.68, 123.71, 119.31, 118.98, 118.29, 114.10, 112.30, 112.18, 102.11, 7, 67.45, 62.01, 60.21, 18.66. HRMS of $[C_{30}H_{23}BrN_4O_4 + Na]^+$ (m/z): 605.0800; Calcd: 605.0778.

*(Z)-1-(4-iodophenyl)-3-(4-(((4-methyl-2-oxo-2H-chromen-**7**-yl)oxy)methyl)-1H-1,2,3-triazol-1-yl)-4-styrylazetidin-2-one* (***10k***)

Yield-83%; mp 238-240 ^{0}C; Cream amorphous solid; IR (neat) (ν_{max}/cm^{-1}): 1758, 1710, 1611, 1385; ^{1}H NMR (400 MHz, $CDCl_3$) δ 7.84 (s, 1H, triazole-CH), 7.67 (dd, *J* = 9.2, 2.1 Hz, 2H, ArH), 7.45 – 7.37 (m, 1H, ArH), 7.29 (d, *J* = 8.8 Hz, 2H, ArH), 7.22 (dd, *J* = 5.0, 1.8 Hz, 3H, ArH), 7.11 (dd, *J* = 6.5, 2.9 Hz, 2H, ArH), 6.83 (dd, *J* = 7.0, 2.3 Hz, 2H, Coumarin-CH), 6.73 (d, *J* = 16.0 Hz, 1H, Vinyl-CH), 6.24 (d, *J* = 5.5 Hz, 1H, Vinyl-CH), 6.13 (d, *J* = 0.9 Hz, 1H, Coumarin-CH), 5.83 (dd, *J* = 16.0, 7.5 Hz, 1H, lactam-CH), 5.22 (d, *J* = 6.7 Hz, 1H, lactam-CH), 5.20 (s, 2H, CH_2), 2.37 (d, *J* = 0.8 Hz, 3H, CH_3). ^{13}C NMR (101 MHz, $CDCl_3$) δ 160.96, 158.51, 138.39, 138.11,

136.43, 134.67, 129.01, 128.70, 126.77, 125.68, 123.68, 119.26, 119.23, 114.11, 112.31, 112.18, 102.12, 89.03, 77.34, 77.02, 76.70, 67.44, 62.01, 60.12, 18.66. HRMS of $[C_{30}H_{23}IN_4NaO_4 + Na]^+$ (m/z): 653.0662; Calcd: 653.0652.

*(Z)-1-(3-chlorophenyl)-3-(4-(((4-methyl-2-oxo-2H-chromen-**7**-yl)oxy)methyl)-1H-1,2,3-triazol-1-yl)-4-styrylazetidin-2-one* (***10l***)

Yield-80%; mp 236-238 ^{0}C;White amorphous solid; IR (neat) (ν_{max}/cm^{-1}): 1758, 1710, 1611, 1388; ^{1}H NMR (400 MHz, $CDCl_3$) δ 7.84 (s, 1H, triazole-CH), 7.50 – 7.45 (m, 2H, ArH), 7.44 – 7.38 (m, 1H, ArH), 7.35 – 7.31 (m, 2H, ArH), 7.24 – 7.20 (m, 3H, ArH), 7.12 (dt, *J* = 7.7, 3.8 Hz, 2H, ArH), 6.86 – 6.80 (m, 2H, Coumarin-CH), 6.74 (d, *J* = 16.0 Hz, 1H, Vinyl-CH), 6.25 (d, *J* = 5.5 Hz, 1H, Vinyl-CH), 6.13 (d, *J* = 1.0 Hz, 1H, Coumarin-CH), 5.84 (dd, *J* = 15.9, 7.4 Hz, 1H, lactam-CH), 5.23 (d, *J* = 6.5 Hz, 1H, lactam-CH), 5.20 (s, 2H, CH_2), 2.37 (d, *J* = 1.0 Hz, 3H, CH_3). ^{13}C NMR (101 MHz, $CDCl_3$) δ 160.95, 158.42, 152.39, 143.52, 138.11, 135.35, 134.69, 130.65, 129.55, 129.01, 128.70, 126.77, 125.67, 123.64, 119.34, 118.67, 114.11, 112.34, 112.13, 102.13, 77.34, 77.02, 76.70, 67.44, 62.03, 60.23, 18.65. HRMS of $[C_{30}H_{23}ClN_4NaO_4 + Na]^+$ (m/z): 561.1306; Calcd: 561.1299.

*(Z)-3-(4-(((4-methyl-2-oxo-2H-chromen-**7**-yl)oxy)methyl)-1H-1,2,3-triazol-1-yl)-1-(3-nitrophenyl)-4-styrylazetidin-2-one* **(*10m*)**

Yield-87%; mp 214-216^{0}C; White crystalline solid; IR (neat) (ν_{max}/cm^{-1}): 1759, 1709, 1611, 1388;^{1}H NMR (400 MHz, $CDCl_3$) δ 8.31 (t, *J* = 2.0 Hz, 1H), 8.03 (dd, *J* = 8.1, 1.6 Hz, 1H), ^{1}H δ 7.91 (d, *J* = 9.4 Hz, 1H, ArH), 7.87 (s, 1H, triazole-CH)., 7.56 (t, *J* = 8.2 Hz, 1H, ArH), 7.42 (d, *J* = 9.3 Hz, 1H, ArH), 7.25 – 7.19 (m, 3H, ArH), 7.14 (dd, *J* = 6.5, 2.8 Hz, 2H, ArH), 6.85 (d, J = 2.8 Hz, 1H, Vinyl-CH), 6.82 (d, J = 5.1 Hz, 2H, Coumarin-CH), 6.31 (d, *J* = 5.0 Hz, 1H, Vinyl-CH), 6.13 (d, *J* = 1.0 Hz, 1H, Coumarin-CH), 5.88 (dd, *J* = 15.9, 7.7 Hz, 1H, lactam-CH), 5.32

(dd, J = 13.1, 7.2 Hz, 1H, lactam-CH), 5.22 (s, 2H, CH_2), 2.37 (d, *J* = 0.8 Hz, 3H, CH_3).^{13}C NMR(101 MHz, $CDCl_3$) δ 160.92, 158.88, 155.04, 152.44, 148.72, 138.96, 137.65, 134.53, 130.54, 129.18, 128.74, 126.85, 125.71, 123.16, 119.86, 118.72, 114.13, 112.34, 112.17, 112.13, 102.11, 67.65, 62.01, 60.74, 18.66. HRMS of $[C_{30}H_{23}N_5NaO_6 + Na]^+$ (m/z): 572.1546; Calcd: 572.1931.

*(Z)-1-(4-chlorophenyl)-3-(4-(((4-methyl-2-oxo-2H-chromen-**7**-yl)oxy)methyl)-1H-1,2,3-triazol-1-yl)-4-styrylazetidin-2-one* (***10n***)

Yield-74%; mp 192-194 ^{0}C; White amorphous solid; IR (neat) (ν_{max}/cm^{-1}): 1759, 1711, 1611, 1384; ^{1}H NMR (400 MHz, $CDCl_3$) δ 7.87 (s, 1H, triazole-CH), 7.59 (t, *J* = 1.9 Hz, 1H, ArH), 7.41 (d, *J* = 8.5 Hz, 1H, ArH), 7.37 – 7.32 (m, 1H, ArH), 7.31 – 7.24 (m, 1H, ArH), 7.24 – 7.20 (m, 3H, ArH), 7.17 – 7.10 (m, 3H, ArH), 6.86 – 6.79 (m, 2H, Coumarin-CH), 6.76 (d, *J* = 16.0 Hz, 1H, Vinyl-CH), 6.26 (d, *J* = 5.4 Hz, 1H, Vinyl-CH), 6.12 (d, *J* = 1.0 Hz, 1H, Coumarin-CH), 5.85 (dd, *J* = 16.0, 7.5 Hz, 1H, lactam-CH), 5.23 (dd, J = 12.9, 6.0 Hz, 1H, lactam-CH), 5.19 (s, 2H, CH_2), 2.36 (d, *J* = 0.9 Hz, 3H, CH_3). ^{13}C NMR (101 MHz, $CDCl_3$) δ 161.15, 160.95, 158.70, 155.03, 152.45, 138.15, 137.79, 135.23, 134.74, 130.51, 128.98, 128.69, 126.80, 125.68, 125.52, 119.34, 117.75, 115.35, 114.09, 112.29, 112.16, 102.09, 77.36, 77.04, 76.72, 67.45, 62.00, 60.32, 18.65. HRMS of $[C_{30}H_{23}ClN_4O_4 + Na]^+$ (m/z): 561.1306; Calcd: 561.1294.

*(Z)-1-(3-methoxyphenyl)-3-(4-(((4-methyl-2-oxo-2H-chromen-**7**-yl)oxy)methyl)-1H-1,2,3-triazol-1-yl)-4-styrylazetidin-2-one* (***10o***)

Yield-85%; mp 167-169 ^{0}C; Brown amorphous solid; IR (neat) (ν_{max}/cm^{-1}): 1757, 1711, 1610, 1384; ^{1}H NMR (400 MHz, $CDCl_3$) δ 7.85 (s, 1H, triazole-CH), 7.45 – 7.37 (m, 1H, ArH), 7.24 – 7.16 (m, 5H, ArH), 7.11 (dd, *J* = 6.5, 2.9 Hz, 2H, ArH), 7.03 – 6.99 (m, 1H, ArH), 6.83 (dd, *J* = 6.6, 2.5 Hz, 2H, Coumarin-CH), 6.77 – 6.70 (m, 2H, Vinyl-CH), 6.23 (d, *J* = 5.4 Hz, 1H, Vinyl-

CH), 6.14 (s, 1H, Coumarin-CH), 5.83 (dd, *J* = 16.0, 7.3 Hz, 1H, lactam-CH), 5.22 (d, *J* = 6.3 Hz, 1H, lactam-CH), 5.20 (s, 2H, CH_2), 3.80 (s, 3H, Ar-OCH_3), 2.37 (d, *J* = 0.8 Hz, 3H, CH_3). ^{13}C NMR (101 MHz, $CDCl_3$) δ 161.16, 160.99, 160.34, 158.58, 152.41, 143.45, 137.91, 137.77, 134.89, 130.26, 128.84, 128.65, 126.75, 125.66, 123.64, 119.76, 114.10, 112.32, 112.13, 111.20, 109.50, 103.59, 102.14, 77.34, 77.03, 76.71, 67.23, 62.05, 60.14, 55.42, 18.65.HRMS of $[C_{31}H_{26}N_4NaO_5 + Na]^+$ (m/z): 557.1801; Calcd: 557.1788.

Materials and methods

Cell culturing

MCF7, A549 and HEK-293 cells were cultured in complete Dulbecco's media Eagle's medium (DMEM) media with 5% FBS and 1% penicillin-streptomycin and MDA-MB-231 cells were cultured in 3:1 DMEM and Ham's F12 with 10% FBS and 1% penicillin-streptomycin, both cell lines were incubated at 37°C and 5% carbon dioxide.

MTT assay Cells were seeded in 96 well plates at a density of 5000 cells per well in triplicate in media. After 24 hours, the test compounds, diluted in complete Dulbecco's media Eagle's medium (DMEM) were added to each well. Cells were treated with a range of different concentrations of drug (1, 5, 10, 20, 50, 100μM) for 24 hours at 37°C and 5% carbon dioxide. For the untreated sample media was used to make up equal volumes. Subsequently, sterile 5μl of 5 mg/mL MTT (Sigma-Aldrich) dissolved in PBS was added to each well and incubated with cells for 2 hours. Solubilisation solution (10% SDS, 10 mM HCl) of equal volume to the wells was then added to each well, which was incubated with cells for 16 hours at 37 °C. The optical density of each well was read at 570 nm using a microtiter plate reader (Thermo Fisher Scientific Multiskan GO Microplate Reader, SkanIt™ software).[38]

Cells were then seeded at a desired density as follows:

$$45\ \mu l \times \text{total no. of wells} = \text{total volume of media required}(\mathbf{a})$$

$$5000\ \text{cells/well} \times \text{total no. of wells} = \text{total no. of cells required}$$

$$\frac{\text{Total volume in flask}(\mu l) \times \text{total no. of cells required}}{\text{Total no. of cells counted in flask}} = \text{volume of cells required from flask}(\mathbf{b})$$

a -b = volume of media to be added to cells

45 µl was then pipetted into each well with 5000 cells per well.

Percentage growth inhibition was calculated as:

100- Treated/Untreated*100

Growth inhibition in untreated sample was considered as 1%

Statistical analysis

The statistical analysis was performed using Excel®, and IC_{50}values were estimated using Graphpad Prism5 software (Hearne Scientific Software). The experiments were performed in duplicate with each concentration run in triplicates, and the statistical significance was calculated using student's t-test. A p-value of less than 0.05 was used to estimate the significance of the observations. A Z-factor was calculated for each 96-well plate and assays having Z-factor above > 0.5 included in the statistical analysis. [39,40]

Methods antimicrobial analysis

Sample preparation

Samples were stored frozen at -20 °C and thereafter prepared in water and DMSO to a final testing concentration of 32 µg/mL or 20 µM (unless otherwise indicated in the data sheet), in 384-well, non-binding surface plate (NBS) for each bacterial/fungal strain, and in duplicate (n=2), and the final DMSO concentration was kept to a maximum of 1% DMSO. All the sample-preparation were

done using liquid handling robots. Compounds that have shown solubility issues during stock solution preparation detailed in the datasheet.

Antimicrobial Assay

Procedure

All bacteria were cultured in Cation-adjusted Mueller Hinton broth (CAMHB) at 37°C overnight. A sample of each culture was then diluted 40-fold in fresh broth and incubated at 37°C for 1.5-3 h. The resultant mid-log phase cultures have diluted (CFU/mL measured by OD600), then added to each well of the compound containing plates, giving a cell density of5´105 CFU/mL and a total volume of 50 µL. All the plates were covered and incubated at 37°C for 18 h without shaking.

Analysis

Inhibition of bacterial growth was determined at an absorbance of 600 nm (OD600), using a Tecan M1000 Pro monochromator plate reader. The percentage of growth inhibition was calculated for each well, using negative control (media only) and positive control (bacteria without inhibitors) on the same plate as references. The significance of the inhibition values determined by modified Z-scores, calculated using the median and MAD of the samples (no controls) on the same plate. Samples with inhibition value above 80% and Z-Score above 2.5 for either replicate (n=2 on different plates)classed as actives. Samples with inhibition values between 50 - 80% and Z-Score above 2.5 for either replicate (n=2 on different plates) classed as partial actives. Samples with inhibition values between 50 - 80% and Z-Score above 2.5 for either replicate (n=2 on different plates) classed as partial actives.[39]

Antifungal Assay

Procedure

Fungi strains cultured for 3 days on Yeast Extract-Peptone Dextrose (YPD) agar at 30°C. A yeast suspension of 1 x 106 to 5 x 106 CFU/mL (as determined by OD530) prepared from five colonies. The suspension subsequently diluted and added to each well of the compound-containing plates giving a final cell density of fungi suspension of 2.5 103 CFU/mL and a total volume of 50 µL. All plates covered and incubated at 35°C for 24 h without shaking.

Analysis

Growth inhibition of *C. albicans was* determined at an absorbance of 530 nm (OD530), while the growth inhibition of *C. neoformans* was determined by the difference in absorbance between 600 and 570 nm (OD600-570), after the addition of resazurin (0.001% final concentration) and incubation at 35 °C for additional 2 h. The absorbance measured using a Biotek Synergy HTX plate reader. The percentage of growth inhibition was calculated for each well, using negative control (media only) and positive control (fungi without inhibitors) on the same plate. The significance of the inhibition values determined by modified Z-scores, calculated using the median and MAD of the samples (no controls) on the same plate. Samples with inhibition value above 80% and Z-Score above 2.5 for either replicate (n=2 on different plates) classed as actives. Samples with inhibition values between 50-80% and Z-Score above 2.5 for either replicate (n=2 on different plates)classed as partial actives.

Antibiotic standards preparation and Quality control

Colistin and Vancomycin were used as positive bacterial inhibitor standards for Gram-negative, and Gram-positive bacteria, respectively. Fluconazole was used as a positive fungal inhibitor standard for *C. albicans and C. neoformans.* The antibiotics were provided in 4 concentrations, 2

above and 2 below its Minimum inhibitory concentration (MIC) value, and plated into the first 8 wells of column 23 of the 384-well NBS plates. The quality control (QC) of the assays determined by the antimicrobial controls and the Z'-factor (using positive and negative controls). Each plate deemed to fulfil the quality criteria (pass QC), if the Z'-factor was above 0.4, and the antimicrobial standards showed the full range of activity, with complete growth inhibition at their highest concentration, and no growth inhibition at their lowest concentration.

Molecular docking

The X-ray crystal structures of estrogen receptor-α (PDB ID: 3ERT) was obtained from the RCSB Protein Data Bank.[41] using the UCSF Chimera package, the ligand and receptor complexes were prepared for docking.[42] Chem3D Ultra was used to construct a three-dimensional structure of ligands. The 3D structure of the 15 tested compounds was further optimised using the force field, MMFF94s in the Avogadro package (V 1.2.0). Auto Dock Tools (V 1.5.6) was used to establish the grid box parameters. All non-polar hydrogens were merged, Gasteiger partial atomic charges added, and rotatable bonds assigned. The grid box of the receptor had a grid spacing of 0.375 Å. The parameters of the grid point are given in **Table 5**. Autodock Vina was used to performing the docking of tested compounds into each of the receptors in triplicate.[43] The docking systems were validated by re-docking the native ligand of the protein crystal structure into the binding site. The Protein-Ligand Interaction Profiler (PLIP) was used to analyze the non-polar interactions between the protein and ligand in complex.[44]

Table 5: Grid point parameters for the docking of test compounds in their respective proteins

GridPoint Parameters	
Grid centre co-ordinates	**Grid size**
X = 30.173	X = 40
Y = -1.997	Y = 30
Z = 24.207	Z = 40

Acknowledgement

The authors thank the Centre for High Computing Performance(CHPC) based in Cape Town (South Africa) for access and use of computational resources. Further thanks are made to the National Research Foundation (NRF-TWAS) South Africa for their financial support toward our research efforts (UID: 99734). "Antimicrobial screening performed by CO-ADD (The Community for Antimicrobial Drug Discovery), funded by the Wellcome Trust (UK) and The University of Queensland (Australia)". Funds provided by NRF (grant no: 109163) to MK for biological activity are also acknowledged.

Author Contribution Statement

P. Singh and Sreekantha B. Jonnalagadda supervised the entire study

S. Dhawan conducted experiments, collected the data and drafted the manuscript.

P. Awolade conducted 2D NMR interpretation.

Ashona-Singh Pillay conducted the computational work.

P. Kisten and N Cele discussed the anti-bacterial screening results.

Sourav. Taru. Saha, and M. Kaur conducted the anti-cancer screening of the compounds, analysed and wrote the corresponding discussion.

Conflicts of Interest

The authors declare no conflict of interest.

References

[1] K. K. Ciombor, C. Wu, R. M. Goldberg, 'Recent Therapeutic Advances in the Treatment of Colorectal Cancer', *Annu. Rev. Med* **2015**, *66*, 83-95. doi:10.1146/annurev-med-051513-102539.

[2] I. J. Higginson, M. Costantini, 'Dying with cancer, living well with advanced cancer', *Eur. J. Cancer* **2008**, *44*, 1414-1424.

[3] N. Kerru, P. Singh, N. Koorbanally, R. Raj, V. Kumar, 'Recent advances (2015–2016) in anticancer hybrids', *Eur. J. Med. Chem* **2017**. doi:10.1016/j.ejmech.2017.07.033.

[4] M. Manav, S. Mohit, S. Abdul, D. Aakash, 'New oxadiazole derivatives of isonicotino hydrazide in the search for antimicrobial agents: Synthesis and in vitro evaluation', *Serb. Chem. Soc* **2012**, *77*, 9-16.

[5] B. Tornimbene, S. Eremin, M. Escher, J. Griskeviciene, S. Manglani, C.L. Pessoa-Silva, 'WHO Global Antimicrobial Resistance Surveillance System early implementation 2016–17', *Lancet Infect. Dis* **2018,** *18*, 241-242. doi:10.1016/S1473-3099(18)30060-4.

[6] H. Wei, J. Ruan, X. Zhang, 'Coumarin-chalcone hybrids: Promising agents with diverse pharmacological properties', *RSC Adv* **2016**, *6*, 10846-10860. doi:10.1039/c5ra26294a.

[7] J. Neyts, E. D. Clercq, R. Singha, Y. H. Chang, A. R. Das, S. K. Chakraborty, S. C. Hong, M. H. Tsay, J. R. Hsu, 'Structure−Activity Relationship of New Anti-Hepatitis C Virus Agents: Heterobicycle−Coumarin Conjugates', *J. Med. Chem* **2009**, *52*, 1486-1490.

[8] J. Dandriyal, R. Singla, M. Kumar, V. Jaitak, 'Recent developments of C-4 substituted coumarin derivatives as anticancer agents', *Eur. J. Med. Chem* **2016**, *119*, 141-68. doi:10.1016/j.ejmech.2016.03.087.

[9] A. Stefanachi, F. Leonetti, L. Pisani, M. Catto, A. Carotti, 'Coumarin: A natural, privileged and versatile scaffold for bioactive compounds', *Molecules* **2018**. doi:10.3390/molecules23020250.

[10] D. N. Nicolaides, K. C. Fylaktakidou, D. J. H. Litina, D. H. Litina, 'Synthesis and biological evaluation of some 4-(isoxazolinyl or 1,2,4-oxadiazolyl) coumarins', *Curr. Pharm. D*es **2004**, *10*, 3813-3826.

[11] P. M. Madalageri, M. Kumar, P. Sachin, Ambekarc , S. Kattimanic , C. Masuku, A. M. Shirahattid, 'Synthesis of 7-carbethoxyamino-4-arylaminomethyl coumarins and their biological studies', *Planta. Med* **2003**, *69*, 1048-1050.

[12] A. R. Quesada, 'Anti-angiogenic drugs: from bench to clinical trials', *Med. Res. Rev* **2006**, *26*, 483–530.

[13] K. Lewis, F. M. Ausubel, 'Mechanism of Persister Formation in Bacteria and Fungi', *Nat. Biotechnol* **2006**, *24*, 1504-1507.

[14] A. Dongamanti, A. Kavitha, V. H. Rao, G. Srinivas, B. Srilata, M. Vijjulatha, 'Microwave-assisted synthesis, molecular docking and antimicrobial activity of novel 2-(3-aryl, 1-phenyl-1H-pyrazol-4-yl)-8H-pyrano [2, 3-f] chromen-4-ones', *Med. Chem. Res* **2016**, *25*, 501-514.

[15] G. L. V. Damu, S. F. Cui, X. M. Peng, Q. M. Wen, G. X. Cai, C. H. Zhou, 'Synthesis and bioactive evaluation of a novel series of coumarinazoles', *Bioorg. Med. Chem. Lett* **2014**, *24*, 3605-3608.

[16] H .G. Ghalehshahi, S. Balalaie, A. Aliahmadi, 'Peptides N-connected to hydroxycoumarin and cinnamic acid derivatives: Synthesis and fluorescence spectroscopic, antioxidant and antimicrobial properties', *New J. Chem* **2018,** *42*, 8831-42. Doi: 10.1039/c8nj00383a.

[17] A. J. Wright, 'The penicillins', *Mayo. Clin. Proc* **1999**, *74*, 290.

[18] M. I. Konaklieva, 'β-Lactams as Inhibitors of Serine Enzymes', *Curr.Med. Chem. Anti-Infect. Agents* **2002**, *1*, 215.

[19] A. Jarrahpour, E. Ebrahimi, E. D. Clercq, V. Sinou, C. Latour, L. D. Bouktab, J. M. Brunel, 'Synthesis of New β-Lactams Bearing the Biologically Important Morpholine Ring and POM Analyses of Their Antimicrobial and Antimalarial Activities', *Tetrahedron* **2011**, *67*, 8699.

[20] M. S. Wilke, A. L. Lovering, N. C. J. Strynadka, 'Beta-lactam antibiotic resistance: a current structural perspective', *Curr. Opn. Microbio* **2005**, *8*, 525-590.

[21] D. Chen, S. C. Falsetti, M. Frezza, V. Milacic, A. Kazi, Q. C. Cui, T. E. Long, E. Turos, Q. P. Dou, 'Anti-tumor activity of N-thiolated beta-lactam antibiotics', *Cancer Lett* **2008**, *63*, 268.

[22] L. Sun, J. Wu, M. Luo, X. Wang, M. Man, Z. Gou, S. D. Dequn, 'Diversity Oriented Design of Various Benzophenone Derivatives and Their in Vitro Antifungal and Antibacterial Activities', *Molecules* **2011**, *12*, 9739-9754.

[23] K. Kushwaha, N. Kaushik, Lata, S.C. Jain, 'Design and synthesis of novel 2H-chromen-2-one derivatives bearing 1,2,3-triazole moiety as lead antimicrobials', *Bioorg. Med. Chem. Lett* **2014**, *24*, 1795-1801.

[24] H. Behbehani, H.M. Ibrahim, S. Makhseed, H. Mahmoud, 'Applications of 2-arylhydrazononitriles in synthesis: preparation of new indole containing 1,2,3-triazole, pyrazole and pyrazolo[1,5-a]pyrimidine derivatives and evaluation of their antimicrobial activities', *Eur. J. Med. Chem* **2011**, *46*, 1813-1820.

[25] X. L. Wang, K. Wan, C. H. Zhou, 'Synthesis of novel sulfanilamide-derived 1,2,3-triazoles and their evaluation for antibacterial and antifungal activities', *Eur. J. Med. Chem* **2010**, *45*, 4631-4639.

[26] K. D. Thomas, A.V. Adhikari, N.S. Shetty, 'Design, synthesis and antimicrobial activities of some new quinoline derivatives carrying 1,2,3-triazole moiety', *Eur. J. Med. Chem* **2010**, *45*, 3803-3810.

[27] N. S. Vatmurge, B.G. Hazra, V.S. Pore, F. Shirazi, M.V. Deshpande, S. Kadreppa, S. Chattopadhyay, R.G. Gonnade, 'Synthesis and biological evaluation of bile acid dimers linked with 1,2,3-triazole and bis-β-lactam', *Org. Biomol. Chem* **2008**, *6*, 3823-3830.

[28] H.C. Kolb, K.B. Sharpless, 'The growing impact of click chemistry on drug discovery', *Drug Discov. Today* **2003**, *8*, 1128-1137.

[29] G. C. Tron, T. Pirali, R. A. Billington, P. L. Canonico, G. Sorba, A. A. Genazzani, 'Click chemistry reactions in medicinal chemistry: applications of the 1,3-dipolar cycloaddition between azides and alkynes', *Med. Res. Rev* **2008**, *28*, 278-308.

[30] P. Singh, S. Kaur, V. Kumar, P. M. S. Bedi, M. P. Mahajan, I. Sehar, H. C. Pal, A. K. Saxena, 'Synthesis and in vitro cytotoxic evaluation of N-alkylbromo and N-alkylphthalimido-isatins', *Bioorg. Med. Chem. Lett* **2011**, *21*, 3017.

[31] S. Maracic, T. G. Kraljevi, S. H. C. Paljetak, M. Peric, M. Matijasic, D. Verbanac, M. Cetina, S. R. Malic, '1,2,3-Triazole pharmacophore-based benzofused nitrogen/sulfur heterocycles with potential anti-Moraxella catarrhalis activity', *Bioorg. Med. Chem* **2015**, *23*, 7448-7463.

[32] S. R. Malic, A. Mescic, 'Recent Trends in 1,2,3-Triazolo-Nucleosides as Promising Anti-Infective and Anticancer Agents', *Curr. Med. Chem* **2015**, *22*, 1462-1499.

[33] S. Korunda, S. Kristafor, M. Cetina, S. R. Malic, 'Design, Synthesis, and the Biological Evaluation of a New Series of Acyclic 1,2,3-Triazole Nucleosides', *Curr. Org. Chem* **2013**, *17*, 1114-1124.

[34] D. Arya, A. Mathur, R. Tyagi, V. Kumar, C. E. Kumar, R. K. Olsen, A. K. Saxena, Prasad 'Chemoenzymatic synthesis of 3'-deoxy-3'-(4-substituted-triazol-1-YL)-5-methyluridine', *Nucleic Acids Res* **2013**, *32*, 646-659.

[35] T. Pirali, S. Gatti, R. D. Brisco, S. Tacchi, E. Zaninetti, E. Brunelli, A. Massarotti, G. Sorba, P. L. Canonico, L. Moro, A. A. Genazzani, G. C. Tron, R. A. Billington, 'Estrogenic Analogues Synthesized by Click Chemistry', *Chem. Med. Chem* **2007**, *2*, 437.

[36] H. V. Pechmann, 'Report of the German chemical society', **1884**, *17*, 929-936.

[37] P. Singh, S. Sachdeva, R. Raj, V. Kumar, M.P. Mahajan, S. Nasser, L. Vivas, J. Gut, P.J. Rosenthal, T.S. Feng, K. Chibale, 'Antiplasmodial and cytotoxicity evaluation of 3-functionalized 2-azetidinone derivatives', *Bioorganic Med. Chem. Lett*. **2011**, *21*, 4561-63. doi:10.1016/j.bmcl.2011.05.119.

[38] S. Sagar, L. Esau, B. Moosa, N. M. Khashab, V. B. Bajic, M. Kaur, 'Cytotoxicity and Apoptosis Induced by a Plumbagin Derivative in Estrogen Positive MCF-7 Breast Cancer Cells', *Anticancer Agents. Med. Chem* **2014**, *14*,170–180.

[39] J. H. Zhang, T. D. Y. Chung, K. R. Oldenburg, 'A Simple Statistical Parameter for Use in Evaluation and Validation of High Throughput Screening Assays', *J. Biomol. Screen* **1999**, *4*, 67-73.

[40] M. Zhuo, 'Noble metals on the nanoscale: optical and photothermal properties and some applications in imaging, sensing, biology, and medicine', *Mol Pain* **2008**, *9*, 44-53.

[41] (http://www.rcsb.org/pdb/home/home.do). Accessed on 22 March 2018.

[42] E. F. Pettersen, T. D. Goddard, C. C. Huang, G.S. Couch, D. M. Greenblatt, E. C. Meng, T. E. Ferrin, 'Molecular Docking of Selective Binding Affinity of Sulfonamide Derivatives as Potential Antimalarial Agents Targeting the Glycolytic Enzymes: GAPDH, Aldolase and TPI', *J Comput Chem* **2004**, *25*, 1605-1612.

[43] O. Trott, A. J. Olson, 'AutoDockVina: improving the speed and accuracy of docking with a new scoring function, efficient optimization, and multithreading', **2010**, *31*,455-461.DOI 10.1002/jcc.21334.

[44] S. Salentin, S. Schreiber, V. J Haupt, M. F. Adasme, M. Schroeder, 'PLIP: fully automated protein-ligand interaction profiler', *Nucleic Acids Res.* **2015**, *1*, 43(W1):W443-7. doi: 10.1093/nar/gkv315.